

# Chem Soc Rev

Chemical Society Reviews

[www.rsc.org/chemsocrev](http://www.rsc.org/chemsocrev)



Themed issue: Smart inorganic polymers

ISSN 0306-0012



**TUTORIAL REVIEW**

C. Viñas *et al.*

Icosahedral boron clusters: a perfect tool for the enhancement of polymer features

**175** YEARS



Cite this: *Chem. Soc. Rev.*, 2016, 45, 5147

Received 1st March 2016

DOI: 10.1039/c6cs00159a

www.rsc.org/chemsocrev

# Icosahedral boron clusters: a perfect tool for the enhancement of polymer features

R. Núñez,<sup>a</sup> I. Romero,<sup>b</sup> F. Teixidor<sup>a</sup> and C. Viñas<sup>\*a</sup>

Boron clusters and organic molecules display manifestly different electronic, physical, chemical and geometrical characteristics. These differences highlight the complementarity of organic synthons and boron clusters, and therefore the feasibility of producing hybrid polymers incorporating both types of fragments. This review focuses on the development of hybrid organic–inorganic  $\pi$  conjugated, silane, siloxane and coordination polymers containing icosahedral boron clusters in the last few decades, which have received considerable academic and technological interest due to the combination of the electronic, optical and thermal properties of traditional inorganic materials with many of the desirable properties of organic plastics, including mechanical flexibility and low production costs.

## Key learning points

- (1) The capability and improved features of both  $\pi$  conjugated and single bond polymers by the inclusion of boron clusters.
- (2) The role of anionic boron clusters as doping agents in producing conductivity in conducting organic polymers (COPs).
- (3) A COP film can self-repair due to a metallocarborane doping agent bonded to the main chain of the polymer.
- (4) Boron clusters usually enhance desired properties in polymers.
- (5) 1D-coordination polymers derived from icosahedral carborane clusters with main group metals, d- and f-block elements.

## Introduction

A polymer is a substance composed of macromolecules; a macromolecule has a high relative molecular mass, with a structure comprising multiple repetition of units derived from molecules of low relative molecular mass. The word polymer comes from the Greek words poly (meaning many) and meros (meaning parts). The molecular structure of a polymer can be linear, branched and cross-linked. The process by which monomers are linked to form polymers is called polymerization. If polymerization takes place without the elimination of any product, the process is called “addition polymerization”, while the process is called “condensation polymerization” if small molecules are eliminated. A large number of organic, inorganic or organometallic compounds can be polymerized. Their physical, chemical and electrical properties depend on complex sets of interacting factors that include molecular structure, molecular size and cross-link density.

Of the many types of polymeric materials,  $\pi$  conjugated organic polymers have attracted much interest because their unusual properties provide them with too many novel applications. Previously, organic polymers were considered good insulators. However, this concept was radically changed when it was shown that the conductivity of polyacetylene can be increased *via* doping by 13 orders of magnitude, up to about  $10^4 \text{ S cm}^{-1}$ . This class of polymers known as electrically conducting organic polymers (COPs) was discovered in 1977 by Alan J. Heeger, Alan G. MacDiarmid and Hideki Shirakawa,<sup>1</sup> who were jointly awarded the Nobel Prize in Chemistry in 2000 “for the discovery and development of conductive polymers”. This was awarded to them for their work on conducting polyacetylene *via* doping with oxidants, which they carried out in the late 1970s. Although there is a large body of research on polyacetylenes, the instability of many of these materials in air, until recently, has limited the number of practical applications. While these studies produced the most dramatic results, investigation of conjugated polymeric materials dates back to the early 1960s, with the first organic polymer of significant conductivity being polypyrrole (PPy) as reported by Donald Weiss and coworkers in Australia.<sup>2</sup> The development of polypyrrole materials is presented beginning with the first report on pyrrole's polymerization in 1915 through the more well-known work of Díaz and coworkers in 1979.<sup>3</sup>

<sup>a</sup> Institut de Ciència de Materials de Barcelona (ICMAB-CSIC), Campus de la U.A.B., E-08193 Bellaterra-Barcelona, Spain. E-mail: clara@icmab.es

<sup>b</sup> Departament de Química, Universitat de Girona, Campus de Montilivi, E-17071 Girona, Spain





Icosahedral boron clusters (Chart 1) display many particular characteristics that are not found in their organic counterparts. The unique stabilities and geometrical properties of the isomeric icosahedral *closo* C<sub>2</sub>B<sub>10</sub>H<sub>12</sub> carboranes in their anionic and neutral forms as well as their exceptional properties, such as low nucleophilicity, unparalleled chemical inertness, electron-withdrawing character through the carbon cluster vertex (C<sub>c</sub>) substituent and adaptable hydrophilicity, have inspired research on the development

of new polymeric materials incorporating boron clusters. Cobaltabisdicarbollide [3,3'-Co(1,2-C<sub>2</sub>B<sub>9</sub>H<sub>11</sub>)<sub>2</sub>]<sup>-</sup> (**1**), which was synthesized in 1965,<sup>4</sup> is the most intensively studied anionic borate cluster, and shows great chemical stability, high molecular volume, low nucleophilic character and low charge density because the negative charge is distributed between 45 atoms.<sup>5</sup>

Icosahedral boron clusters are part of polymeric structures linked by C<sub>c</sub> or by B atoms through covalent two-centered-two-electron



**R. Núñez**

Rosario Núñez was born in Loja (Granada), Spain, in 1968. In 1991 she graduated in Chemistry at Universidad de Granada. In 1994 she received her MSc degree in Chemistry at Universitat Autònoma de Barcelona (UAB). She carried out her thesis at Inorganic Materials & Catalysis Laboratory (LMI) at the Materials Science Institute of Barcelona (ICMAB-CSIC) under the supervision of Prof. Clara Viñas and received her PhD from UAB

in 1996. After that, she worked as a postdoctoral fellow with Prof. Bruno Boury and Robert Corriu at Université de Montpellier II. In 1999, she joined the ICMAB as a fellow staff doctor to work in the LMI managed by Prof. Francesc Teixidor. Since 2001 she has a permanent position as a tenured scientist. Her research interests are the synthesis and study of properties of boron cluster derivatives, and preparation of carboranyl-containing molecular and hybrid materials.



**I. Romero**

M. Isabel Romero García (1966, Alcaraz) graduated in Chemistry at the University of Murcia in 1989; she obtained her PhD in Chemistry from the Universitat Autònoma de Barcelona (UAB) in 1995. After post-doctoral studies at the Laboratoire de Electrochimie Organique et Photochimie Redox (CNRS, Université Joseph Fourier Grenoble) under the supervision of Professors Alain Deronzier and M. Noëlle Collomb, she obtained a position

as a lecturer of chemistry at the University of Girona (UdG) in 2001. Her research interests involve the synthesis and study of transition metal complexes to be used as potential catalysts for sustainable and environmentally friendly processes. In the last few years, she has been interested in the study of complexation of boron clusters to cheap metals such as Cu, Mn, Fe or Co, in collaboration with Professors Francesc Teixidor and Clara Viñas.



**F. Teixidor**

Francesc Teixidor obtained his PhD in Chemistry in 1979 from Universitat Autònoma de Barcelona under the supervision of Prof. Heribert Barrera and pursued postdoctoral research with Prof. Ralph Rudolph at the University of Michigan. He was appointed Assistant Professor at Universitat Autònoma de Barcelona in 1982. In 1987 he got an Associate Professor position at the Spanish Council for Scientific Research (CSIC) at the

Materials Science Institute (ICMAB). Since 1999 he has held a Full Professor position at the same Institute. His research interests are in the chemistry, particularly in the formation of B-C and B-P bonds, and application of boron cluster compounds in molecular materials with particular emphasis on energy.



**C. Viñas**

Prof. Clara Viñas graduated in Chemistry at the Universitat Autònoma de Barcelona in 1975 and in Pharmacy at the Universitat de Barcelona in 1980. She worked as a pre-doctoral student at the Prof. Rudolph's Laboratory at The University of Michigan for a year. Back to Barcelona, she worked for industry and later moved to Laboratori Municipal de Sabadell where she became the director to work on food and environmental control. She got her PhD in

Pharmacy under the supervision of Prof. F. Teixidor at the Universitat de Barcelona in 1990. She joined the staff of the C.S.I.C. as a Tenured Scientist in 1991. She was promoted to research scientist in 2002 and to research professor in 2006. Her research interests are in the synthesis of novel boron compounds, carboranes and metallocarboranes, to be used for future medicinal applications.





**Chart 1** Icosahedral heteroboranes with their vertex numbering: *closo*  $[B_{12}H_{12}]^{2-}$ , *closo*  $[CB_{11}H_{12}]^{-}$ , *nido*  $[C_2B_9H_{12}]^{-}$ , isomers of *closo*  $C_2B_{10}H_{12}$  carboranes (*ortho*-(1,2), *meta*-(1,7), and *para*-(1,12)) and metallacarboranes  $[3,3'-M(1,2-C_2B_9H_{11})_2]^{-}$ ,  $M = Co(III)$  in (1) and  $M = Fe(III)$  in (2). Pink circles correspond to B–H vertices while the grey circles to C–H vertices.

( $2c-2e^{-}$ ) bonds. However, these clusters have the capacity to produce three-centered-two-electron ( $3c-2e^{-}$ ) bonds, given the hydride character of the H atoms of the B–H vertices. Thus, coordination polymers with icosahedral boron clusters as ligands are important for their potential applications as well as from their structural chemistry perspective.

Since the discovery of polyhedral boranes in the early 1960s, new inorganic–organic hybrid boron cluster-containing polymers (polypyrrole, polythiophene, silane, siloxane–acetylene, polyaryl(ether), polyimides, ...) have been developed to combine, in a single polymeric system, the desirable features of inorganic materials such as high-temperature stability, hardness and chemical inertness with easy processability and high solubility characteristics of organic materials.

The trend towards miniaturization of devices and, at the same time, improved performance, high reliability and ease of use shows that electronic and semiconductor industries are constantly demanding more technically advanced and sophisticated materials. This review aims to present the current status of hybrid polymers incorporating icosahedral boron clusters and how the new polymers present enhanced properties. We are confident that the review will be of great practical value to both boron cluster scientists and researchers in other areas that are interested in exploring the possibilities of boron clusters. Hopefully it will also increasingly find its way into advanced teaching, showing the possibilities of boron clusters to the future new scientists.

## I. Conducting organic polymers incorporating icosahedral boron clusters

COPs are also known as “synthetic metals” because of their potential application as substitutes for metals or inorganic semiconductors. COPs are promising materials for technological and biomedical applications due to their attractive electronic and optical properties. Conducting and reducing

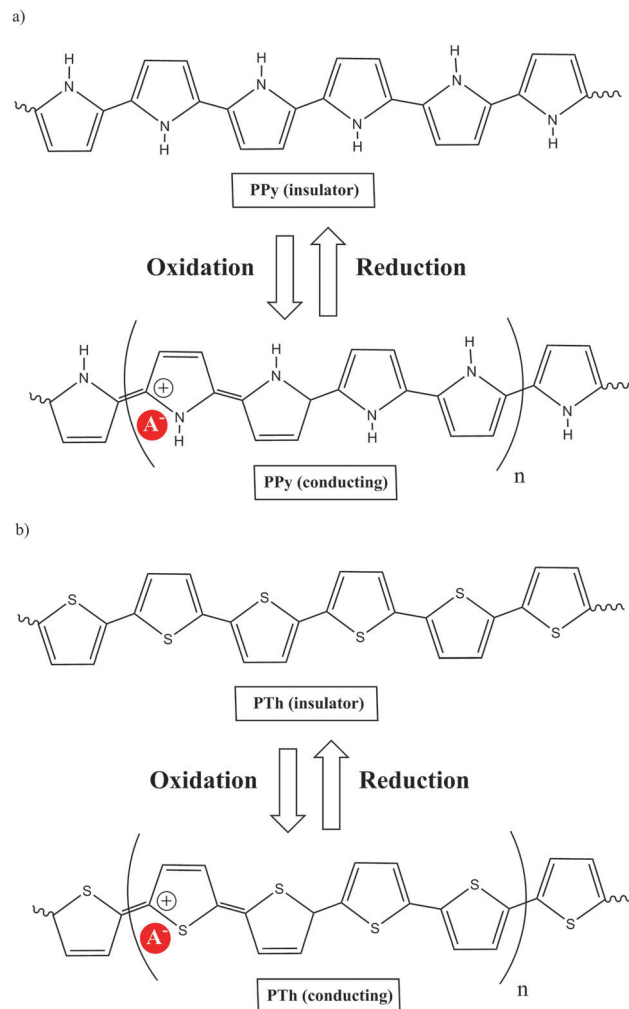


**Fig. 1** Conducting and insulating states generated electrochemically. (a) PPY; (b) PTh.

states of COPs can be easily electrochemically generated from the corresponding monomers. During electropolymerization, anions from the solution are inserted into the polymer matrix to maintain the material's electroneutrality, neutralizing the positive charges generated in the oxidized polymer threads (Fig. 1). The conducting state of COPs is the one requiring a doping agent and is produced by oxidizing the insulating material.

Doping agents play a relevant role in the stability, morphology as well as in the chemical and physical properties of the polymer. Therefore, the nature of the counter-ion used in electropolymerization and the applied experimental conditions play a very important role in the resulting properties of the COP films.  $[ClO_4]^{-}$ ,  $Cl^{-}$ ,  $[BF_4]^{-}$ ,  $[PF_6]^{-}$ ,  $[NO_3]^{-}$ , surfactants such as dodecylbenzene sulfonate (DBS), dodecyl sulfonate, naphthalene sulfonate, and even counter-ions like heteropolyanions ( $[SiW_{12}O_{40}]^{4-}$  or phosphotungstate  $[PW_{12}O_{40}]^{3-}$ ), among others have been studied as doping agents. For practical applications, long-term stability of the material towards repetitive oxidation/reduction cycling or towards exposure to high anodic potential for short



periods of time is of primary interest. A major obstacle to the commercialization of COPs is the relatively poor stability of the COP-based devices to several degradation mechanisms such as rapid oxidation by water or oxygen, by Joule heating or by volume change when the oxidation state of the material is changed electrochemically.<sup>6</sup>

The chemical stability limit of COPs is known to be related to the overoxidation resistance limit (ORL) of the material, beyond which the properties of the conducting material are definitely lost. COPs have been made more resistant to overoxidation by doping with low nucleophilic, low electron density and low coordinating hydrophobic anions.

Boron clusters have been built into the electroactive polymers with the following main objectives: (i) to play the role of a doping agent (Sections 1a and 3); (ii) to modify the chemical composition of the COPs by the doping agent (Section 1.1b) or (iii) to incorporate boron into the polymer (Sections 1.2b and 2). The first step to achieve the preparation of novel COPs covalently linked to neutral or anionic icosahedra boron cluster derivatives is the synthesis of the starting monomer derivatives covalently bonded to the corresponding boron cluster. The second step is the electropolymerization of these functionalized monomers to produce the corresponding COP films.

### 1. Polypyrrole materials containing icosahedral boron clusters

Of the many COPs, polypyrrole (PPy) is one of the most popular. Chemical methods for the oxidative polymerisation of pyrrole

had been known for many years, but a new era in the development of these materials arose when Diaz produced the first free-standing films of electrochemically deposited polypyrrole, poly-*N*-methylpyrrole and poly-*N*-phenylpyrrole on platinum electrodes in a  $\text{CH}_3\text{CN}/[\text{NEt}_4][\text{BF}_4]$  solution.<sup>3</sup>

The electrochemical formation of conductive PPy films takes place by the anodic oxidation of pyrrole in  $\text{CH}_3\text{CN}$  at a moderate positive potential ( $E_{1/2} = 1$  to  $1.3$  V vs. Saturated Calomel Electrode (SCE)). The initially formed radical species is immediately oxidized at the applied potential, since it is more oxidizable than the monomer, leading to a new radical cation. The continuing reaction is a lengthening of the oligomer chain. Since polymers from pyrrole have markedly lower oxidation potentials (0 to  $0.4$  V (SCE)) than the monomer, they are obtained in an oxidized state which is electrically conducting, allowing the growth of the film. The important point is that the resulting polymer contains mainly structural units linked to 2,5 positions of the pyrrole ring (Chart 2). Thus, non-substituted pyrrole at the 2,5 positions is highly recommended to produce good quality PPy films.

**1a. Polypyrroles that incorporate boron clusters as doping agents of electroactive polymers.** The first described PPy that incorporates anionic icosahedral boron clusters as doping agents was announced in 2000, when the PPy electrochemical synthesis of pyrrole ( $0.1$  M) in the presence of  $3.5 \times 10^{-2}$  M in Cs(1), with 1% (v/v) water was reported.<sup>7</sup> Electropolymerization was performed in  $\text{CH}_3\text{CN}$  in a double compartment cell with a standard three-electrode system; Pt, Pt wire and Ag/AgCl ( $0.1$  M  $[\text{NBu}_4]\text{Cl}$  in  $\text{CH}_3\text{CN}$ ) were used as working, counter and reference electrodes, respectively. Sequential cyclic voltammograms for the electropolymerization of pyrrole in the presence of (1) displayed a continuous growth of the PPy(1) film after every new cycle proving the conducting nature of the formed material (Fig. 2).<sup>7</sup> Besides, the anodic and cathodic semicycles present precisely well-defined peaks (Fig. 2a). The PPy(anion) abbreviation would mean, through this review text, the polypyrrole polymer doped with the anion that appears in the parenthesis.

Due to the hydrophobicity, large size and multiple binding properties of the anion (1), its retention within the polymeric

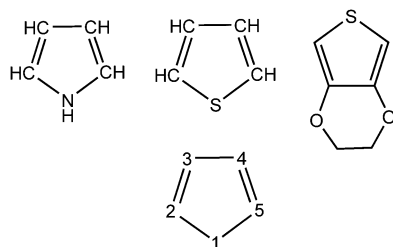


Chart 2 Pyrrole, thiophene and dioxithiophene monomers and the pentagonal cycle vertex numbering.

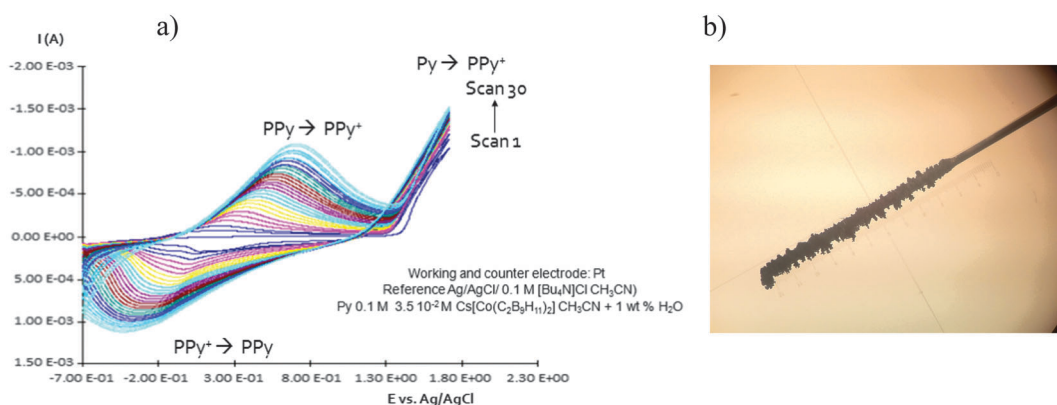


Fig. 2 (a) Homogeneous and continuous intensity increases after each cycle. (b) Pt electrode after growing during twenty cycles PPy with Cs(1) as a doping agent.







**Scheme 1** The oxidation–reduction process in PPy(1) occurs *via* de-insertion and insertion of cations: acting the material as a cation exchanger.

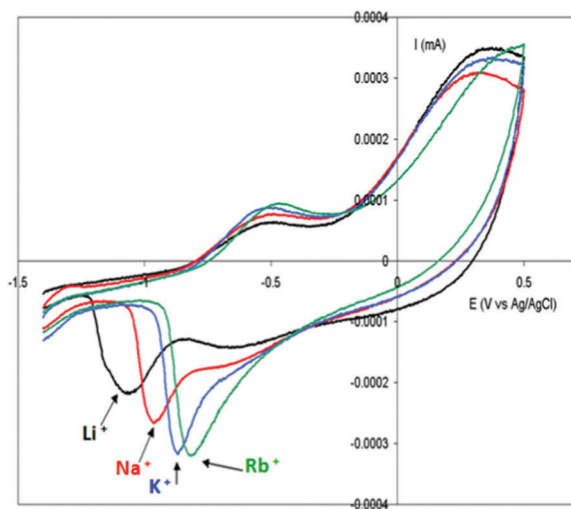


**Fig. 3** Cyclic voltammetry of PPy(1) membranes in aqueous alkaline chlorides: LiCl 0.1 M; NaCl 0.1 M; KCl 0.1 M; RbCl 0.1 M; CsCl 0.1 M. Scan rate of electrode potential 20 mV s<sup>-1</sup>.

PPy(1) material is facilitated. Thus, the oxidation–reduction process, also called doping/undoping, occurs *via* de-insertion and insertion of cations (Scheme 1). The PPy(1) film is highly sensitive to the cationic volume of the solute, allowing the development of cationic selective membranes by control of the applied reducing potential (Fig. 3). The chronocoulometries registered during the charge–discharge process show an almost perfect reversibility of the cation exchange process and no detectable degradation of the membrane due to (1) loss or overoxidation even after 40 successive cycles.

To study if PPy(1) interacted with the large cations of alkylammonium and phosphonium salts, cyclic voltammetry was performed on PPy(1) in either aqueous solutions of [NR<sub>4</sub>]Cl, or [PR<sub>4</sub>]Cl.<sup>8</sup> The materials were made of a conducting PPy(1) covered by a layer of well-adhered crystals of [NR<sub>4</sub>]<sup>+</sup> or [PR<sub>4</sub>]<sup>+</sup> salts that were observed by SEM. Although the layers resemble self-assembled monolayers (SAM), there are noticeable differences between the two types of surface coatings; particularly the



**Fig. 4** Graphical representation of the PPy(1) polymer modified by [NBu<sub>4</sub>]<sup>+</sup> and [PBu<sub>4</sub>]<sup>+</sup>.

cationic species participate in the generation of the layer even though there is no possible way to covalently bind the cations to the PPy surface. These stable layers, which can be made of variable compactness, are the result of the formation of [NR<sub>4</sub>][(1)] or [PR<sub>4</sub>][(1)] salts that are highly insoluble in water. Fig. 4 graphically shows the material. The films, which are unidirectional (inwards) cation barriers, are highly stable in aqueous media but are easily dissolved in CH<sub>3</sub>CN in which the [NR<sub>4</sub>][(1)] or [PR<sub>4</sub>][(1)] salts are soluble.<sup>8</sup> This discovery can be of remarkable interest both as a new way to deposit crystalline materials layers on the surface of COP films, and also as a way of producing defects on the surface by the controlled removal of the doping anions.

Recently, the surface functionalization of a Pt electrode by the electropolymerization of pyrrole doped with the anionic *closo* ferrabisdicarbollide cluster, [3,3'-Fe(1,2-C<sub>2</sub>B<sub>9</sub>H<sub>11</sub>)<sub>2</sub>]<sup>-</sup>, (2), has been reported. As in the above described case of PPy(1) films, the doping agent (2) allows PPy(2) to grow without limits increasing its conductivity after each cycle.

The in-depth uniform distribution of the doping anion (1) was unambiguously demonstrated in PPy(1) films by using X-ray photoelectron spectroscopy (XPS) analysis and argon ion sputtering with no special experimental difficulties, thanks to the high boron content of PPy(1). XPS measurements provided a surface polymer composition of C<sub>5.3</sub>N<sub>1</sub>B<sub>4.15</sub>Co<sub>0.23</sub>, corresponding to a PPy/(1) ratio of 4.3. Moreover, the high-energy N<sup>+</sup> shoulder is about 22% of the total N(1s) signal, in agreement with the previous results.<sup>7</sup> Bearing in mind the above findings, further geometrical calculations confirmed the Py/(1) ratio stoichiometry. A graphical display of the ideal view of the PPy(1) layers is shown in Fig. 5. The B–B diameter of the B–B longest distance in (1) is ≈11.0 Å including the two hydrogen atoms. Simple calculations performed on the unit [H–Py–Py–Py–H]<sup>2+</sup> show that the farthest two carbon atoms are separated by ≈12.3 Å, relatively close to the axial H–(B)⋯(B)–H distance in (1). From a geometrical point of view, there are 4 pyrrole fragments per each (1) anion.<sup>9</sup>

PPy materials doped with the anionic icosahedral boron clusters: [B<sub>12</sub>H<sub>12</sub>]<sup>2-</sup> (3) and [B<sub>12</sub>I<sub>12</sub>]<sup>2-</sup> (4);<sup>10</sup> [1-NH<sub>3</sub>-B<sub>12</sub>H<sub>11</sub>]<sup>-</sup> (5), [1-NH(CH<sub>2</sub>-C<sub>6</sub>H<sub>5</sub>)<sub>2</sub>-B<sub>12</sub>H<sub>11</sub>]<sup>-</sup> (6), [1-NH(CH<sub>2</sub>-C<sub>10</sub>H<sub>7</sub>)<sub>2</sub>-B<sub>12</sub>H<sub>11</sub>]<sup>-</sup> (7) and [1-NH(CH<sub>2</sub>-C<sub>12</sub>H<sub>23</sub>)<sub>2</sub>-B<sub>12</sub>H<sub>11</sub>]<sup>-</sup> (8);<sup>10</sup> as well as monoanionic metallocarborane derivatives of (1): aryl (9)–(12),<sup>10</sup> polyether



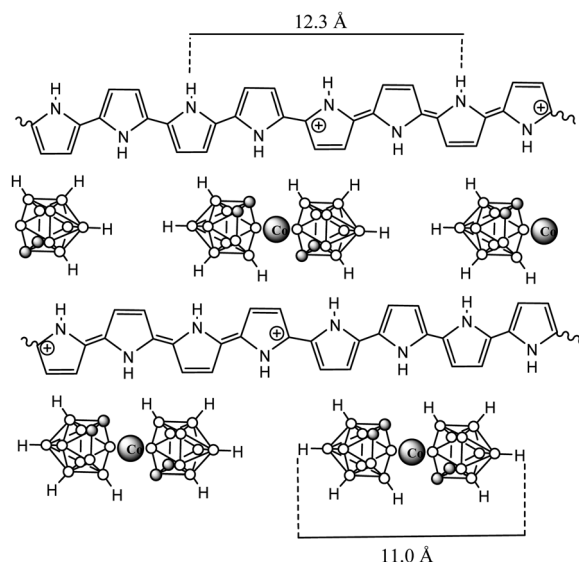


Fig. 5 Graphical representation of the PPy(1) polymer.

(13)–(14)<sup>10</sup> and polyTHF (15)–(16) were also reported to study the influence of different composition (metallacarborane or borane), shape (*commo* bisdicarbollide or icosahedron) and charge (one or two) as well as different substituents (at the boron vertex or at the carbon one) of the doping icosahedral boron anions on the film growth and the ORL value (Table 1). Charts 3 and 4 display the chemical structure of these anions.

The PPy film growth speed found was PPy(1) > PPy(11) > PPy(12) > PPy(9) > PPy(10). The materials with less tendency to grow are PPy(13) and PPy(14); their growth is one order of magnitude less than for PPy(1). When doping agents were (13)–(16), the conductivity decays dramatically after each new cycle until flattening the signal. This indicates higher difficulty in the materials' growth and consequently a very thin layer on the electrode. Polyether and polyTHF branches of the monomers (13)–(14) and (15)–(16) beam away from the surface, not allowing the deposition of new polymer layers, and therefore ceasing the material growth.

As SEM displayed different morphologies between PPy(1) and common anion doped PPy(ClO<sub>4</sub>) and PPy(PF<sub>6</sub>) membranes (Fig. 6), the ORL and thermal resistance of these materials were studied.<sup>10</sup> ORL tests (Fig. 7a) were carried out by linear sweep

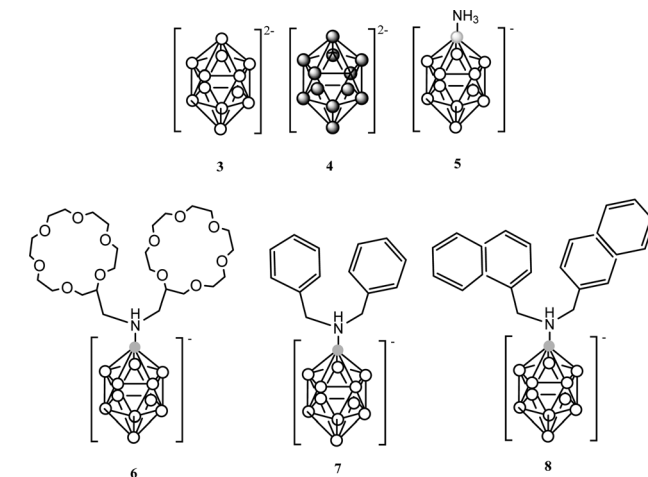


Chart 3 Chemical structures of the [B<sub>12</sub>H<sub>12</sub>]<sup>2−</sup> (3) and its derivatives (4)–(8). White circles correspond to B–H while the dark circles to B–I vertices and the grey circles to a B atom.

voltammetry (LSV). A higher ORL value of the PPy(1) material, approx. 300 mV, as compared to commonly used doping anions, (ClO<sub>4</sub>) and (PF<sub>6</sub>), was obtained. The overoxidation stability of PPy(1) was attributed to the unique capacity of (1) to continuously compensate the moving positive charges in the COP layer (Fig. 5). The tridimensional disposition of B–H's in (1) is ideal to cover all points in space, therefore having the ability to completely compensate the cationic charge of the PPy film. ORL values of PPy(1)–PPy(14) membranes are summarized in Table 1.

Furthermore, thermogravimetric analysis (TGA) in an inert atmosphere shows that the presence of (1) improves the thermal resistance of the PPy increasing both the temperature at which the weight loss begins (200 °C vs. 130 °C) and the temperature at which the weight loss completes, up to 600 °C (22% vs. 36%).<sup>7</sup>

The enhanced ORL and thermal properties of these PPy(1)–PPy(14) materials have opened up significant opportunities for their application in practical devices. The fate of the doping anions before and during the polymer overoxidation processes was studied.<sup>10</sup> Fig. 8 shows the XPS studies of the plain, anodically processed, PPy(7) material and its overoxidized sample. The chemical composition on C and B of the plain PPy(7) film remains unaltered throughout the whole thickness of the sample (Fig. 8a). Conversely, its overoxidized sample

Table 1 ORL values (in volts) of different PPy films doped with anionic icosahedral shape boron clusters, PPy(1)–PPy(17); PPy films containing icosahedral boron clusters doped with [PF<sub>6</sub>]<sup>−</sup> compared to PPy polymers doped with common anions

Compound	ORL (in volts)	Compound	ORL (in volts)
PPy(1)	1.257	PPy(12)	1.33 <sup>10</sup>
PPy(3)	0.91 <sup>10</sup>	PPy(12)	1.33 <sup>10</sup>
PPy(4)	0.96 <sup>10</sup>	PPy(13)	1.41 <sup>10</sup>
PPy(5)	0.99 <sup>10</sup>	PPy(14)	1.45 <sup>10</sup>
PPy(6)	1.15 <sup>10</sup>	PPy(17) copolymer	No observation of a defined peak in the range 0–1.8 V <sup>5</sup>
PPy(7)	0.90 <sup>10</sup>	PPy(PF <sub>6</sub> )	0.89 <sup>7</sup>
PPy(9)	1.21 <sup>10</sup>	PPy(DBS)	0.93 <sup>7</sup>
PPy(10)	1.15 <sup>10</sup>	PPy(ClO <sub>4</sub> )	0.9 <sup>5</sup>
PPy(11)	1.27 <sup>10</sup>		





**Chart 4** Chemical structures of the anionic metallabisdicarbollides (**1**) and (**2**) and its derivatives (**9**)–(**18**). White circles vertices correspond to B–H while the dark circles to C<sub>c</sub>–H vertices and grey circle to B atom.

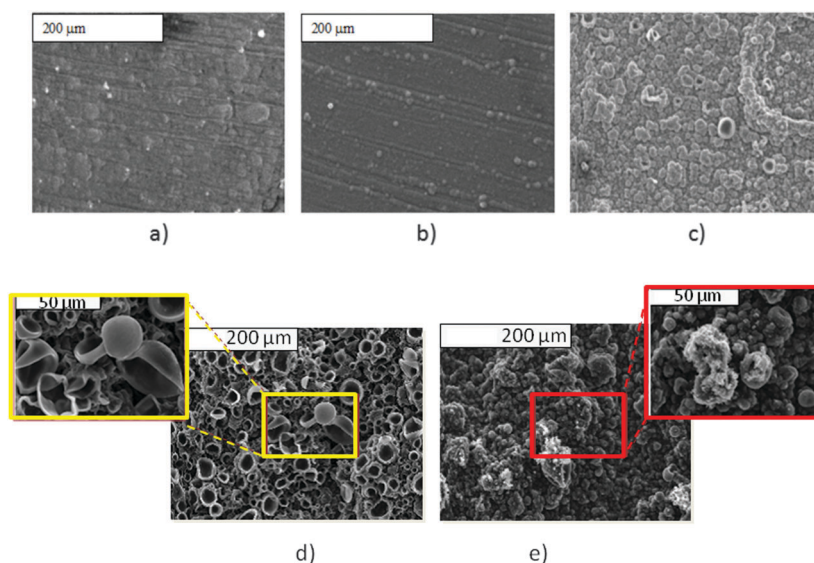


**Fig. 6** S.E.M. studies of PPy films doped with different anions: (a) PPy(ClO<sub>4</sub>); (b) PPy(DBS); (c) PPy(**1**) and its surface modification by [NBu<sub>4</sub>]<sup>+</sup> and [PBU<sub>4</sub>]<sup>+</sup>, (d) and (e) respectively. (Fig. 6d reproduced with permission from ref. 8. Copyright 2002, John Wiley and Sons).

(Fig. 8b) shows two distinct regions: in the inner layers region (horizontal lines) boron atomic concentration is lower than expected for a homogeneous overoxidized film whereas layers close to the solution membrane face (vertical lines) show a higher concentration. This can be understood as the movement of the doping anion during the overoxidation process from the inner layers (closer to the electrode) to the solution membrane surface (Fig. 9).<sup>10</sup>

**1b. Polypyrroles that incorporate boron clusters at the branches of the polymer.** Pyrrole derivatives covalently linked to carborane or metallacarborane clusters can be synthesized

by bonding the substituent at the β carbon atoms of the pyrrole ring, 3-, 3,4-, or at the N-vertices of the pyrrole ring (Chart 2).

**1b.1. N-Substituted pyrrole units incorporating anionic closo-cobaltabisdicarbollide.** Following the ring opening reaction,<sup>4</sup> pyrrole rings covalently bonded at the N- by a diether aliphatic chain to an anionic cobaltabisdicarbollide unit [3,3'-Co(8-C<sub>4</sub>H<sub>4</sub>N-(CH<sub>2</sub>)<sub>2</sub>-O-(CH<sub>2</sub>)<sub>2</sub>-O-1,2-C<sub>2</sub>B<sub>9</sub>H<sub>10</sub>)(1',2'-C<sub>2</sub>B<sub>9</sub>H<sub>11</sub>)]<sup>-</sup> (**17**) and [3,3'-Co(8-C<sub>4</sub>H<sub>4</sub>N-(CH<sub>2</sub>)<sub>5</sub>-O-1,2-C<sub>2</sub>B<sub>9</sub>H<sub>10</sub>)(1',2'-C<sub>2</sub>B<sub>9</sub>H<sub>11</sub>)]<sup>-</sup> (**18**) were obtained as pyrrole substituted synthons for the preparation of COPs.<sup>11</sup>





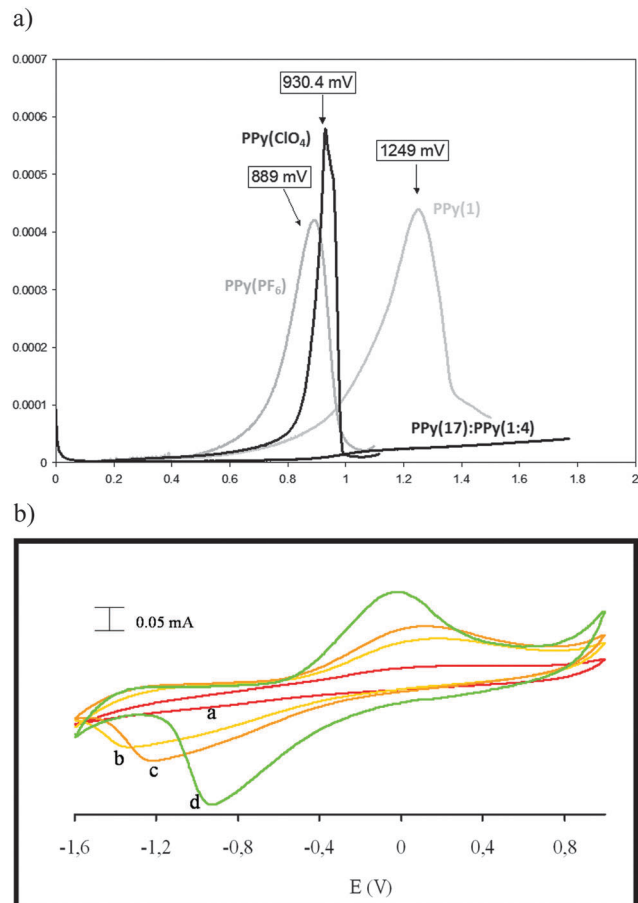


Fig. 7 (a) LSV studies of PPy(PF<sub>6</sub>), PPy(ClO<sub>4</sub>), PPy(1) and copolymer PPy(17):PPy (1:4). LSV consists of the measurement of the current associated with overoxidation during a single scan (0 to 1.5 V vs. Ag/AgCl) at low scan rate (0.5 mV s<sup>-1</sup>) in a 0.5 M KCl solution. (b) Gradual self-repairing of copolymer PPy(17):PPy shown by ion exchange tests in NaCl 0.1 M: (a) immediately after destabilizing the PPy(17):PPy by applying 1300 mV, (b) after 30 minutes in the same electrolytic solution, (c) after 1 h and (d) after 18 h.

The polymerization of the anionic monomer (17) as well as its copolymerization with pyrrole units leads to the formation of a new group of self-doped PPy(17) and copolymer PPy(17):PPy,<sup>5</sup> improving the already outstanding properties



Fig. 9 The different steps of the overoxidation process: (a) doping anions migration; (b) doping anion accumulation at the surface; (c) doping anion expulsion due to its hydrophobic character. The zig-zag lines stand by the PPy chains while grey circles represent the positions of the doping anions and the empty circles the previously occupied position and the arrows indicate the trajectory of the moved anion. (Reproduced with permission from ref. 10. Copyright 2005, Elsevier).

previously described by PPy(1).<sup>7</sup> Fig. 10 displays the proposed structure of PPy(17) and its copolymer PPy(17):PPy (1:4). As the doping agent is inherently bonded to the pyrrole unit in compound (17), no supporting electrolyte is necessary during polymerization. So, the electropolymerization of K(17) was carried out in dry CH<sub>3</sub>CN by cycling the potential from -0.5 to 1.7 V vs. Ag/AgCl/[N(C<sub>4</sub>H<sub>9</sub>)<sub>4</sub>]Cl (0.1 M CH<sub>3</sub>CN). Fig. 11(a) shows the growth of PPy(17). Copolymerization of (17) with a pyrrole monomer (ratio 1:1) was carried out under the same conditions indicated above (Fig. 11b). Higher current intensities and a lower half wave potential were found in the copolymer PPy(17):PPy with respect to the polymer PPy(17), suggesting the existence of longer chains and a better packing of polymeric chains in the copolymer PPy(17):PPy. As is known, the introduction of large groups into the pyrrole ring at the *N*- or 3-position usually brings about a drop in the conductivity and an increase of the band gap due to the steric hindrance to planarity of the conjugated system.<sup>5</sup> This is not the case of (17). The conductivity

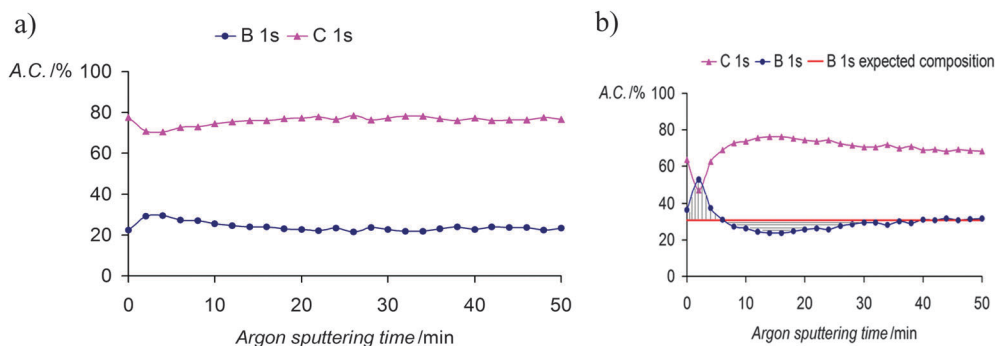


Fig. 8 (a) XPS studies of PPy(7) membrane and (b) XPS studies of the overoxidized PPy(7) material. The membrane was set so that the side in contact with the solution is the first to be sputtered. (Reproduced with permission from ref. 10. Copyright 2005, Elsevier).

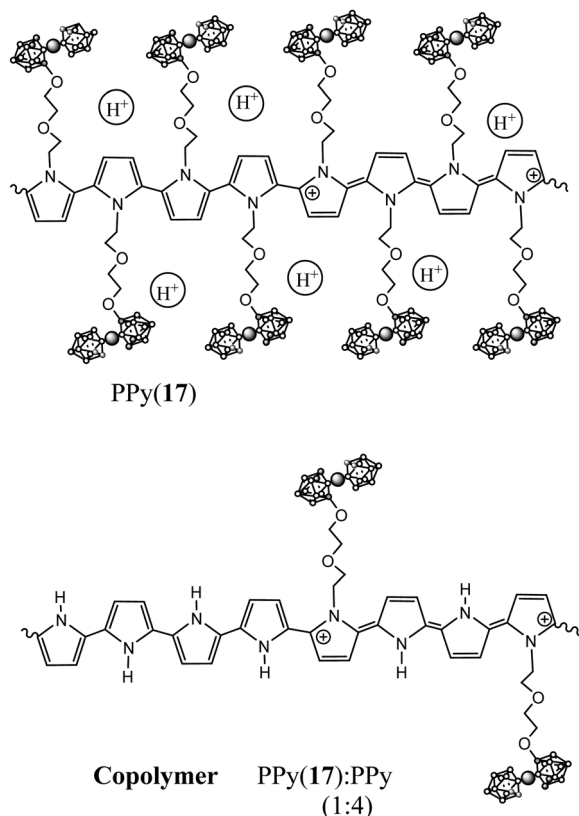


Fig. 10 Proposed structures of the polymer PPy(17) and its copolymer (1 : 4) PPy(17) : PPy.



Fig. 11 Potentiodynamic curves obtained for (a) polymerization of monomer (17). (b) Copolymerization of compound (17) with pyrrole (1 : 1). (Reproduced with permission from ref. 5. Copyright 2002, John Wiley and Sons).

of thin PPy(17) films and the PPy(17):PPy copolymer was measured by the four-point probe method and was found to be 1 and 9 S  $cm^{-1}$ , respectively.<sup>5</sup> Common anion doped PPy(Cl) or PPy(ClO<sub>4</sub>)

prepared under the same conditions show conductivities in the same order of magnitude than the copolymer.

Combining plasma argon ion sputtering and XPS, it was found that the PPy(17) composition is practically constant through the whole depth of the material indicating the absence of chain defects during electrochemically film growth and that one charge carrier exists nearly every four pyrrole units ( $N^+/N_{total}$  ratio  $\sim 0.25$ ) as for PPy(1).<sup>5</sup> The amount of  $K^+$  found in the polymer matrix was negligible so, the threefold excess of (17) anions were compensated by  $H^+$  generated during the polymerization process, which were trapped into the PPy(17) film (Fig. 10).

ORL experiments of the self-doped copolymer PPy(17):PPy do not show a clear maximum suggesting an extraordinary increase of its overoxidation resistance (Fig. 7a).<sup>5</sup> Thus, for compositionally similar materials, copolymers PPy(17):PPy and PPy(1), the fact that (1) is grafted to the PPy strand allows the copolymer PPy(17):PPy to go far beyond the overoxidation limit of the PPy(1) that has no anion grafting. The self-doped copolymer PPy(17):PPy is the best PPy material in terms of overoxidation resistance. The copolymer PPy(17):PPy can be a remarkable example of a self-repairing material because the material really does not degrade upon overoxidation because the reversible overoxidized  $\leftrightarrow$  reduced process is permitted and in the case that the overoxidation threshold was surpassed the material would react to restore itself (Fig. 7b).<sup>12</sup> This unique behavior is due to grafting of the cobaltabisdicarbollide (1) to the PPy but also depends on the nature of the anion.<sup>12</sup>

Because monomer (17) had inhibited the polypyrrole backbone oxidation in the films of PPy(17), copolymerization of monomer (17) with the cationic water-oxidation catalyst  $[Ru_2(\mu-bpp)(tpp)_2(H_2O)_2]^{3+}$ , (bpp = bis(2-pyridyl)pyrazolato anion and ttp = 4'-(p-pyrrolylmethylphenyl)-2,2':6',2''-terpyridine), was done by electropolymerization of solutions containing a 1 : 1 molar ratio of both monomers in a fluorine-doped tin oxide electrode (FTO).<sup>13</sup> The ratio of monomers incorporated into the PPy backbone of the material was evaluated by UV/vis spectroscopy and turned out to be roughly 1 : 1, indicating that the rate of polymerization of both monomers is practically the same. The newly generated material, the copolymer PPy(17) and  $[Ru_2(\mu-bpp)(tpp)_2(H_2O)_2]^{3+}$  on the FTO surface, is capable of oxidizing water to molecular dioxygen with a turnover number (TN) of 250. This value represents the best performance ever obtained in a heterogeneous phase using a chemical oxidant.<sup>13</sup>

**1b.2. C-Substituted pyrrole synthons bonded to carborane clusters.** 3- and 3,4-pyrrole derivatives covalently linked to a neutral *clos*o or anionic *nido o*-carborane via a methylene or ethylene spacer have been synthesized. These synthons (see Chart 5) are as follows: (i) neutral mono-substituted (19),<sup>14</sup> (20),<sup>14</sup> (21),<sup>15</sup> (22),<sup>15</sup> (ii) neutral di-substituted (23),<sup>16</sup> (24)<sup>15</sup> and (iii) anionic mono-substituted compounds (25),<sup>14</sup> (26).<sup>14</sup>

The first conducting polymer functionalized with covalently linked carborane units was obtained by anodic oxidation of the substituted (19) pyrrole monomer in  $10^{-1}$  M  $[NBu_4][PF_6]$  anhydrous  $CH_3CN$ .<sup>17</sup> The electrosynthesis of PPy20( $PF_6$ ) films was carried out from  $10^{-2}$  M solution of (20) under the same

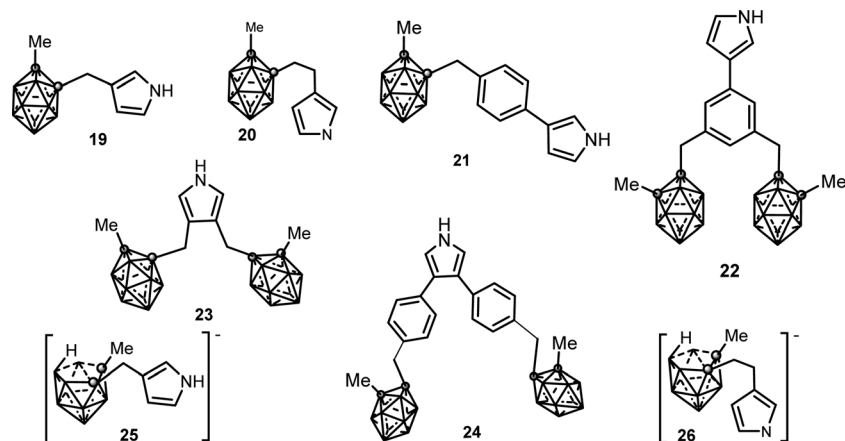


**Chart 5** Chemical structures of the monosubstituted (19)–(22) and disubstituted (23) and (24) neutral pyrroles, as well as the anionic (25) and (26) ones. Vertices correspond to B–H while the circles to the C<sub>c</sub> atom.

conditions. Monomer (20) that presents an ethyl group spacer was more efficiently electropolymerized than (19) with a methylene group. The charge transport mechanism across the films was controlled by the diffusion of (PF<sub>6</sub>) counteranions. The resulting electroactive PPy19(PF<sub>6</sub>) and PPy20(PF<sub>6</sub>) films exhibit strongly increased overoxidation resistance, about 120<sup>17</sup> and 300<sup>14</sup> mV respectively, shifted towards more positive potentials compared with plain PPy(PF<sub>6</sub>). The conductivity ( $\sigma \sim 10^{-1}$  S cm<sup>-1</sup>) of the PPy19(PF<sub>6</sub>) polymer, measured at room temperature by the four-probe method, is 2–3 orders of magnitude lower than that of other 3-monosubstituted polypyrroles.<sup>17</sup> These electrochemical characteristics were directly attributable to the presence of the carboranyl moiety: its increased ORL is due to the electron-withdrawing character of the carboranyl unit while decreased conductivity is a consequence of the steric bulkiness of the carborane cluster, which would produce conformational constraints in the conjugated backbone decreasing its mean conjugation length.<sup>17</sup>

Moreover, these PPy19(PF<sub>6</sub>) and PPy20(PF<sub>6</sub>) materials were more thermally stable than PPy(PF<sub>6</sub>); only 15% loss in the mass was found for PPy19(PF<sub>6</sub>) at 700 °C while a continuous mass loss up to 70% was observed for PPy(PF<sub>6</sub>). The improvement was attributed to the oxidation of B–H vertices of the carboranyl cluster to the more thermally stable B–O–B groups.<sup>14</sup>

The oxidation of (21) and (24) monomers led to the formation of the PPy21(PF<sub>6</sub>) and PPy24(PF<sub>6</sub>) films. The disubstituted 3,5-pyrrole (24) and its corresponding PPy24(PF<sub>6</sub>) polymer were oxidized at a more positive potential than the substituted 3-pyrrole (21) and its conforming PPy21(PF<sub>6</sub>) membrane due to the presence of two sterically hindered carborane clusters at the 3,5-vertices of the pyrrole ring (Table 1).

However, when comparing PPy23(PF<sub>6</sub>) and PPy24(PF<sub>6</sub>), the poly(3,4-diphenylpyrrole) PPy24(PF<sub>6</sub>) was found to be more easily oxidizable which indicates a more conjugated structure, as was also supported by the UV-vis spectroscopy data.<sup>15</sup> The monosubstituted monomer (22) that contains two carboranyl clusters did not yield a conducting polymer deposit even under a different set of experimental conditions (oxidation potentials, solvents, monomer concentration, among others), possibly due

to the high steric hindrance of the dicarboranylmethylphenyl substituent at the 3-position of the pyrrole ring.<sup>15</sup>

In contrast with the feasible anodic electropolymerization of the neutral carboranyl pyrrole units, the anionic pyrrole synthons (25)<sup>14</sup> and (26) were found to not electropolymerize under the tested experimental conditions.<sup>14</sup> At 0.1 V s<sup>-1</sup>, two closely spaced irreversible redox processes were observed for both monomers (0.50/0.82 V and 0.48/0.75 V, respectively vs. Ag/Ag<sup>+</sup> 10<sup>-2</sup> M). For the first redox system, the number of electrons involved in the rate-determining step was two while in the second redox process the results were perfectly consistent with one-electron transfer.<sup>14</sup> While the nature of these two irreversible redox systems was not fully elucidated, their low values are consistent with the oxidation of the anionic *nido* carboranyl cluster because the oxidation of the pyrrole unit requires higher potentials. In addition, no visible film was detected on the electrode surface in the range 0.8–1.5 V vs. Ag/Ag<sup>+</sup> 10<sup>-2</sup> M.<sup>14</sup>

The ability of the anionic *N*-substituted pyrrole (17) to electropolymerize is to be noted, in contrast to the non-electropolymerization of the anionic pyrrole synthons (25),<sup>14</sup> and (26) described below.<sup>14</sup>

## 2. Polythiophene materials containing icosahedral boron clusters

Thiophene is a heterocyclic compound (Chart 2) consisting of a flat five-membered ring. The polythiophene polymer (PTh) is formed by linking the monomers through their 2,5 positions and become electrically conductive upon partial oxidation. The current thiophene derivatives (Chart 6) incorporating the neutral *closo* or anionic *nido* carborane cage covalently linked to 3- or 3,4-thiophene moieties or *via* a phenyl spacer arm are as follows: (i) neutral mono- and di-substituted (27),<sup>15</sup> (28),<sup>15</sup> (30), (31), (32),<sup>18</sup> (34),<sup>19</sup> and (ii) anionic mono-substituted (29)<sup>15</sup> and (33).<sup>19</sup>

Efficient electropolymerization of neutral (30), (31) and (32) monomers was performed in CH<sub>2</sub>Cl<sub>2</sub> + 0.2 M [NBu<sub>4</sub>][PF<sub>6</sub>]. As the (30)–(32) units have one  $\alpha$  ring carbon directly linked to the C<sub>c</sub> of carborane cage, the PTh30(PF<sub>6</sub>)–PTh32(PF<sub>6</sub>) COPs contain





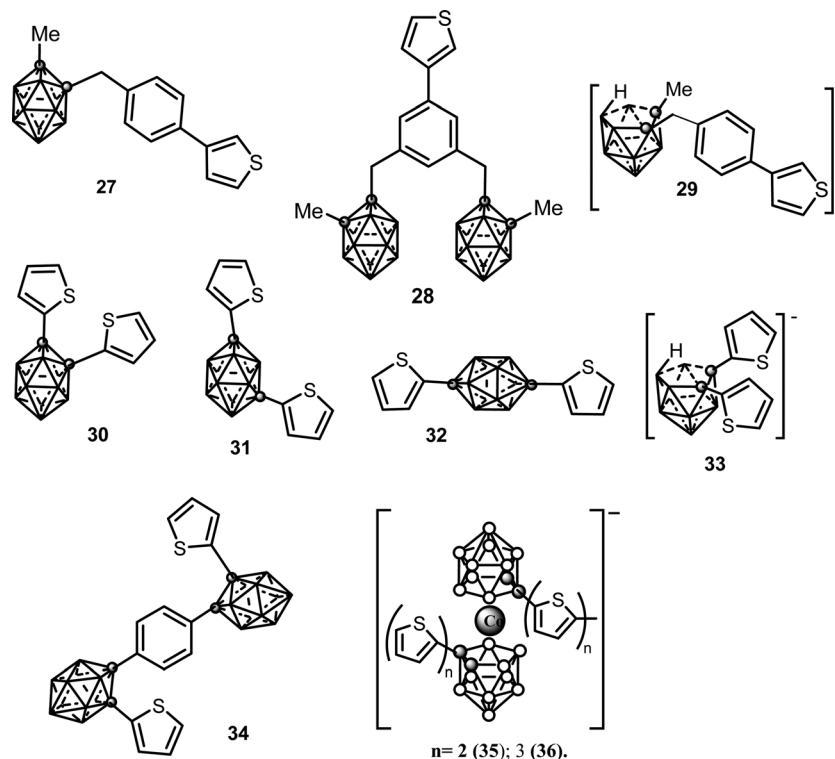


**Chart 6** Chemical structures of the monosubstituted neutral (27), (28), (30)–(33), (34) and anionic (29), (33), (35) and (36) thiophenes. Vertices correspond to B–H while the circles to the C<sub>6</sub> atom.

the carborane clusters in the polymer backbone. These polymers show high thermal and electrochemical stabilities compared to parent PThs. The PThs30(PF<sub>6</sub>) has the highest doping level, which is associated with the formation of the largest population of bipolaron charge carriers that largely reduce the  $\pi$ – $\pi^*$  band gap and provide the highest conductivity of this family of materials. In the insulating form, PTh30(PF<sub>6</sub>)–PTh32(PF<sub>6</sub>) films display optical features at 528, 488 and 425 nm, respectively. PTh30(PF<sub>6</sub>) shows a well defined fine structure of high conjugation.<sup>18</sup>

There is no effect on the electroactivity of PTh27(PF<sub>6</sub>) and PTh28(PF<sub>6</sub>) when highly oxidizing potentials are applied.<sup>15</sup> No COPs were generated from monomers (29), (33) and (34).<sup>19</sup> Polythiophene films, PTh35(PF<sub>6</sub>) and PTh36(PF<sub>6</sub>), containing in-chain (1) covalently linked to two bithienyl and terthienyl units were prepared by electropolymerization in CH<sub>3</sub>CN. These films display redox processes attributed to the p-doping/undoping of the expected quaterthienyl and sexithienyl segments at *ca.* 0.8 V *vs.* SCE. PTh35(PF<sub>6</sub>) and PTh36(PF<sub>6</sub>) display a more extended degree of conjugation than the parent oligothiophenes indicating a significant electronic delocalization through the cobaltabisdicarbollide cluster. These materials were efficient for the electrocatalytic reduction of protons to H<sub>2</sub> suggesting them to be robust and efficient catalysts.

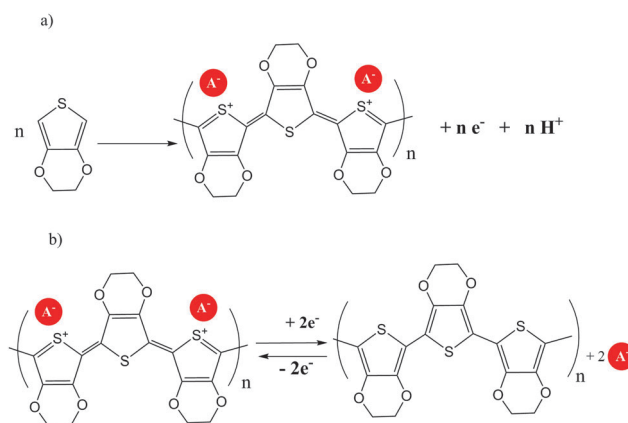
### 3. Poly(3,4-ethylenedioxythiophenes) containing icosahedral boron clusters

Conductive polymers like poly(3,4-ethylenedioxythiophene) (PEDOT) are very attractive due to their outstanding properties: extremely

stable and highly conductive state; high transparency (90% at *d* = 100 nm) and flexibility; high chemical and thermal/UV stability; easy processing by polymer dispersion as ready-to-use formulations mixed with solvents and additives or “*in situ*” monomer polymerization for industrial scale production.

Commonly, the monomer ethylene dioxythiophene (EDOT) is converted into a polymer (PEDOT) through oxidative polymerization (Scheme 2).

Despite the outstanding physico-chemical applications of PEDOT doped as a COP, the studies of PEDOT either with metallocarboranes or carboranes are lacking. The first report



**Scheme 2** (a) Electropolymerization process of EDOT to produce PEDOT. (b) Polymer reduction reaction for PEDOT.



on PEDOT(metallacarborane) was published in 2006.<sup>20</sup> The electropolymerization of EDOT on indium tin oxide (ITO) from Cs(1) in CH<sub>3</sub>CN solution gave the polymer PEDOT(1) that is accompanied by a reversible oxidation of the doping anion. It results in a p-doped polymer embedded with short-chain reduced oligomers, as proven by the material composition, morphology, electrochemical and spectroelectrochemical behavior. The ratio between the numbers of EDOT molecules entrapped in the polymer vs. the oligomers is 0.88. This ratio was estimated from the doping level of the material considering that only the polymer can be doped. Its oxidation/reduction process takes place reversibly in the potential range  $-0.8/+0.7$  V vs. SCE and is accompanied by cation exchange due to the non-extrudable character of the doping anion (1). It was also shown that an important oligomeric fraction is embedded in the main polymer.<sup>20</sup>

Recently, new electrochromic copolymers of EDOT and 1,7-(2'-(SC<sub>4</sub>H<sub>3</sub>)<sub>2</sub>-1,7-carborane (31) were synthesized, characterized and their electro-optical properties were reported.<sup>21</sup> Several copolymers PEDOT(31):PEDOT were successfully prepared from various monomer feed ratios by electropolymerization. Electrochemical and optical properties of the copolymers can be adjusted by playing with monomer feed ratios; the maximum wavelength of PEDOT at 600 nm can be shifted to lower values (*i.e.*, 522 nm) by increasing the ratio of (31) in the monomer mixture. The copolymer films showed electrochromic properties: purple when reduced and transparent sky blue when oxidized. Also, during redox switching the films exhibited a percent transmittance change between 32% and 46% with a switching time between 1.0 s and 1.3 s.<sup>21</sup>

## II. Photoluminescent carborane-containing $\pi$ -conjugated polymers

All conjugated polymers possess extended  $\pi$  conjugation through the molecular backbone alternating double and single bonds that produce a delocalization of the  $\pi$  electrons across all adjacent aligned p-orbitals. Single and double bonds become similar and  $\pi$ -electrons can be readily moved from one bond to the next, which makes conjugated polymers one-dimensional semiconductors. Excitation energies of conjugated  $\pi$  electrons are usually in the visible range and they are, therefore, addressed as being optically active. One of the drawbacks for these  $\pi$  conjugated polymers is the extended conjugation through aromatic moieties that have a tendency to bundle and  $\pi$ -stack. These phenomena influence the processability and stability of such systems, which limits their utilization in optoelectronic devices. The incorporation of carborane clusters into the polymers' backbone or branches aids to confer solubility and stability, while altering their luminescence properties.

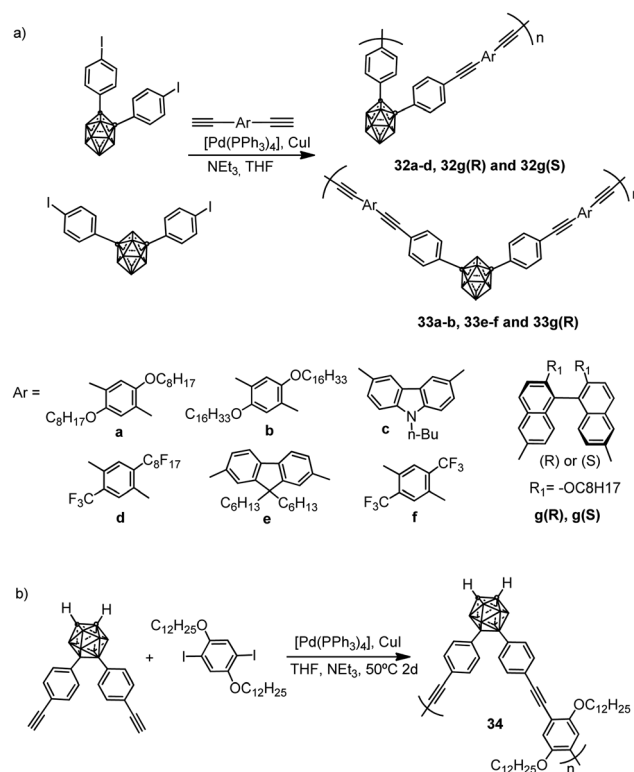
### 1. Carborane-containing *p*-phenylene-ethynylene-based polymers (PPE)

Several examples of molecular  $\pi$  conjugation of icosahedral [CB<sub>11</sub>Cl<sub>10</sub>]<sup>−</sup> clusters and *exo*-2D  $\pi$  systems have been recently reported.<sup>22,23</sup> Different families of  $\pi$ -conjugate polymers containing

*o*-, *m*- and *p*-carborane (Chart 1) in the backbone have been reported during the last few years.<sup>24</sup> The incorporation of aromatic and carboranyl groups into the backbone produces a stabilizing effect but, additionally, linear  $\pi$ -conjugate aryl-ethynyl-carborane polymers exhibit photoluminescence properties.

$\pi$ -Conjugate polymers 32a-d, 33a-b, 33e-f and chiral  $\pi$ -conjugate polymers 32g(R)-33g(R) and 32g(S) were synthesized from the reactions of monomer bis(4-iodophenyl)-*o*-carborane or bis(4-iodophenyl)-*m*-carborane with the corresponding *p*-phenylene-ethynylene derivatives by a Sonogashira-Hagihara coupling polycondensation reaction (Scheme 3a). Polymer 34, in which the *p*-phenylene-ethynylene units are bonded at B9 and B12 atoms, was also prepared (Scheme 3b). The number-average molecular weights ( $M_n$  in g mol<sup>−1</sup>) of 32a-d, 32g(R) and 32g(S) were 2800, 3100, 4100, 3200, 3800 and 3000, respectively, whereas polymers 33a-b, 33e-f, 33g(R) and 34 displayed higher molecular weights of 26 600, 27 600, 36 400, 31 200, 29 800, respectively. The obtained polymers were soluble in organic solvents such as THF, CHCl<sub>3</sub>, CH<sub>2</sub>Cl<sub>2</sub> and toluene.

Polymers 32a-c and 32g(R) were not fluorescent in THF solutions due to an intramolecular charge-transfer (CT) process from the electron-donating *p*-phenylene-ethynylene units to the antibonding orbital of the C<sub>c</sub>-C<sub>c</sub> bond in *o*-carborane. In contrast, their homologous with *m*-carborane 33a-b, 33e-f and 33g(R), as well as polymer 34 shows intense blue emission in CHCl<sub>3</sub> (Table 2). In 34, the inclusion of substituents at the B vertices of the *o*-carborane cluster does not cause any structural change in the excited state of the *p*-phenylene-ethynylene moiety so its



Scheme 3 (a) Polymers with *o*- and *m*-carborane linked by C<sub>c</sub>; (b) polymers with *o*-carboranyl linked by the B<sub>c</sub>.



Table 2 Photophysical properties of polymers

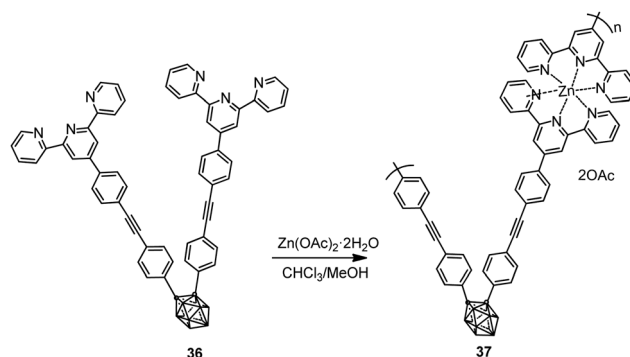
Compound					
Compound	CB isomer	Solvent	$\lambda_{\text{abs}}$ (nm)	$\lambda_{\text{em}}$ (nm)	$\phi_{\text{F}}$
32a	<i>ortho</i>	THF	379	559 <sup>a</sup>	3.8 <sup>a</sup>
32b	<i>ortho</i>	THF	380	550 <sup>a</sup>	n.d.
32c	<i>ortho</i>	THF	358	583 <sup>a</sup>	n.d.
32d	<i>ortho</i>	THF	345	405	n.d.
33a	<i>meta</i>	CHCl <sub>3</sub>	314, 378	415	0.25
33b	<i>meta</i>	CHCl <sub>3</sub>	314, 378	415	0.25
33e	<i>meta</i>	CHCl <sub>3</sub>	319, 362	386, 410	0.11
33f	<i>meta</i>	CHCl <sub>3</sub>	345, 366	409	0.22
32g(R)	<i>ortho</i>	THF	241, 283, 338	566 <sup>a</sup> (562) <sup>b</sup>	0.05 <sup>a</sup> (0.23) <sup>b</sup>
33g(R)	<i>meta</i>	THF	239, 292, 335	388 (562) <sup>b</sup>	0.50 (0.09) <sup>b</sup>
34	<i>ortho</i>	CHCl <sub>3</sub>	413 <sup>b</sup>	403	0.38
35a	<i>ortho</i>	THF	312, 375	411, 430	0.51
35b	<i>ortho</i>	THF	353, 368	383, 410	0.40
36	<i>ortho</i>	CHCl <sub>3</sub> -CH <sub>3</sub> OH	314	440	<0.002
37	<i>ortho</i>	CHCl <sub>3</sub> -CH <sub>3</sub> OH	334	465	0.18
38	<i>ortho</i>	THF	428	471 (529) <sup>a</sup>	n.d.
40	<i>ortho</i>	Chlorobenzene	550 (543) <sup>b</sup>	n.d.	n.d.
41	<i>ortho</i>	Chlorobenzene	784 (793) <sup>b</sup>	n.d.	n.d.
43	<i>para</i>	CHCl <sub>3</sub>	n.d.	400	n.d.
45a	<i>ortho</i>	CHCl <sub>3</sub>	384 <sup>c</sup>	423 (563) <sup>b</sup> (565) <sup>c</sup>	n.d.
45b	<i>ortho</i>	CHCl <sub>3</sub>	441 <sup>c</sup>	602 (570) <sup>b</sup>	n.d.
47	<i>ortho</i>	n.d.	n.d.	535 <sup>d</sup>	n.d.
48	<i>ortho</i>	n.d.	n.d.	535 <sup>d</sup>	n.d.
49	<i>Me-ortho</i>	n.d.	292, 330, 341	351, 366	n.d.
50	<i>Ph-ortho</i>	n.d.	292, 330, 341	—	n.d.

<sup>a</sup> Measured in THF/H<sub>2</sub>O (1/99) (v/v) at room temperature. <sup>b</sup> Thin film. <sup>c</sup>  $\lambda_{\text{max,edge}}$ . <sup>d</sup> Thin films before and after annealing for 3 h at 160 °C.

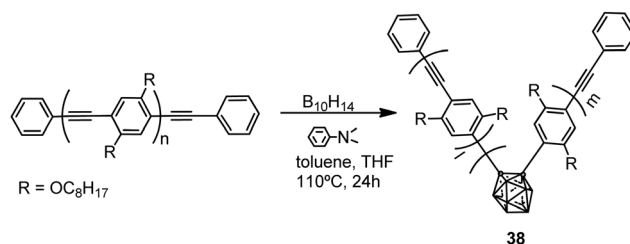
luminescence is not affected. Nevertheless, polymers **32a–c** and **32g(R)** exhibited orange emission in suspensions of THF/H<sub>2</sub>O, 1/99 (v/v) (Table 2), which originated from aggregation-induced emission (AIE). Additionally, **32g(R)** and **33g(R)** films showed fluorescence emission bands at 562 nm (Table 2), indicating that the carborane unit prevents the stacking of  $\pi$ -conjugated main chains.

Following the same Sonogashira–Hagihara polycondensation procedure aromatic ring-fused carborane-based  $\pi$ -conjugated polymers **35a** and **35b** were synthesized (Scheme 4).<sup>25</sup> Contrarily to polymers **32a–c**, **35a** and **35b** exhibited intense blue luminescence in THF solution (Table 2). The introduction of benzo-carborane has little effect on the intramolecular cage- $\pi$  interaction in the excited state, thus the carborane cage acts as a simple electron-withdrawing group without disturbing the emission of  $\pi$ -conjugated systems.

Polymer **37** was also synthesized by complexation of ligand **36** with Zn(OAc)<sub>2</sub>·2H<sub>2</sub>O via Sonogashira–Hagihara coupling reaction (Scheme 5).<sup>26</sup> While monomer **36** was not luminescent in solution, polymer **37** exhibited fluorescence with an emission maximum at 465 nm (Table 2).

Scheme 5 Synthesis of polymer **37**.

Polymers with the structure of **38** were obtained by the reaction of *nido*-decaborane (B<sub>10</sub>H<sub>14</sub>) with the poly(*p*-phenylene-ethynylene) polymer in different ratios (0.05, 0.10, 0.20, 0.40) (Scheme 6). The *M<sub>n</sub>* of **38** decreases from 4600 to 3200 with increasing feed ratio.<sup>27</sup> These polymers showed light blue emission

Scheme 4 Synthesis of benzocarborane fused polymers **35**.Scheme 6 Synthesis of polymer type **38** using B<sub>10</sub>H<sub>14</sub>.



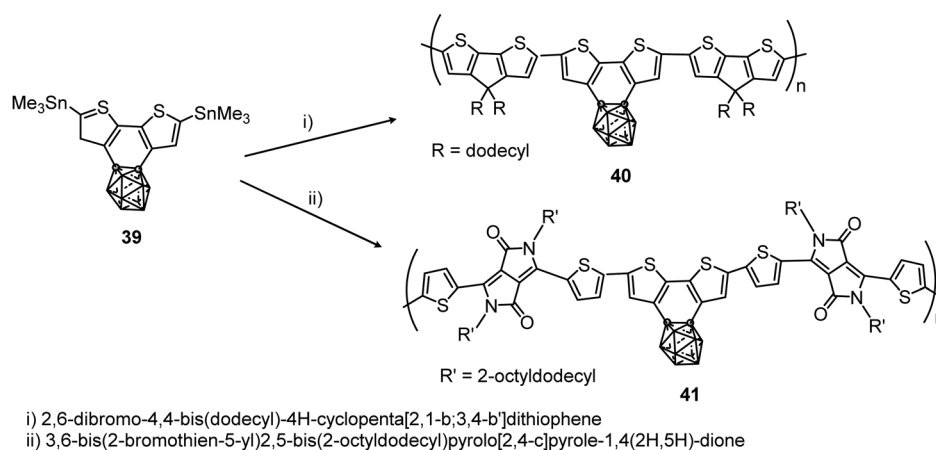
in THF, whereas in the solvent mixture THF/H<sub>2</sub>O, 1/99 (v/v) the emission maximum was red-shifted to 529 nm, indicating a shortening of the effective  $\pi$ -conjugation length due to the introduction of carborane clusters (Table 2). Furthermore, the introduction of the *o*-carborane clusters into the polymer main chain led to a high thermal resistance and an improvement in ceramic yields upon thermolysis to 1050 °C.

More recently, the polymerization of benzocarborene-[2,1-*b*:3,4-*b'*]dithiophene (**39**) to give polymers **40** and **41** with the aromatic ring fused to the carborane cluster has been reported (Scheme 7).<sup>28</sup> These polymers showed excellent thermal stability with  $T_{d5}$ , which is the temperature at which the polymer

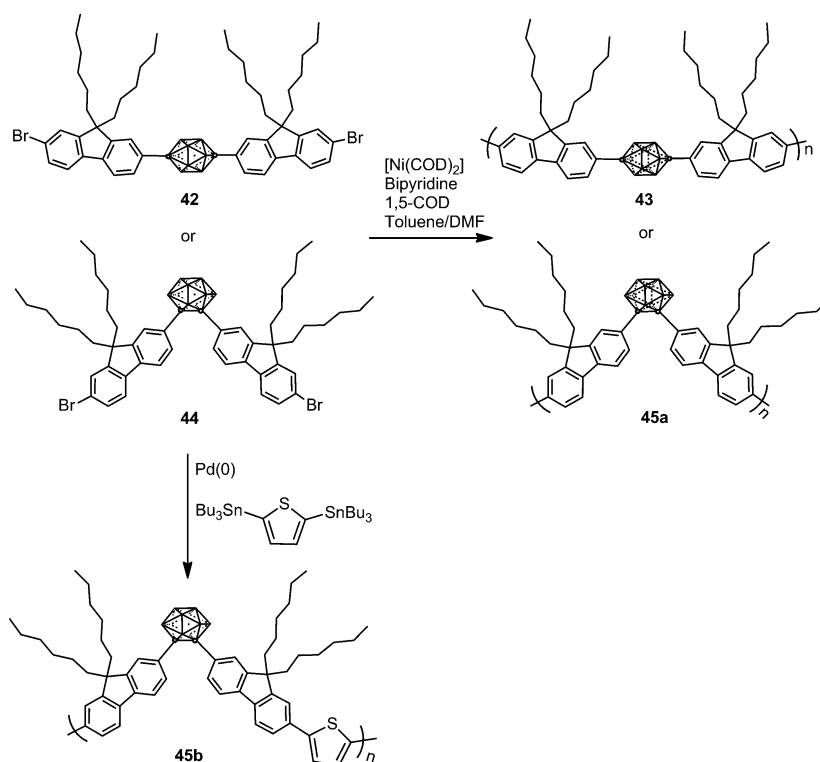
loses 5% of its weight, at above 375 and 400 °C, respectively. Absorption data of **40** and **41** in solution and films are given in Table 2. The ionization potentials of these polymers were 5.0 and 5.4 eV, slightly larger than polymers without carboranes, indicating that the cluster acts as an inductive electron-withdrawing comonomer.

## 2. Carborane-containing polyfluorene polymers

In 2009, *p*- and *o*-carborane-containing polyfluorene polymers **43** and **45a** were synthesized from **42** and **44**, respectively, using a Yamamoto type Ni(0) dehalogenative reaction in the presence of [Ni(COD)<sub>2</sub>] (Scheme 8).<sup>29</sup> Later, polymer **45b** was obtained *via*



Scheme 7 Microwave assisted preparation of polymers **40** and **41** at 200 °C for 30 min in the presence of [Pd<sub>2</sub>(dba)<sub>3</sub>] and P(*o*-tol)<sub>3</sub> in chlorobenzene.



Scheme 8 Synthesis of polymers **43**, **45a** and **45b**.



a Stille coupling reaction as shown in Scheme 8.<sup>30</sup> The thermal analysis of polymers **45a** and **45b** showed a glass transition temperature ( $T_g$ ) between 128 and 137 °C.

Polymer **43** exhibits blue emission in  $\text{CHCl}_3$ , whereas the presence of *o*-carborane in **45a** gave an additional second band, red-shifted, at around 565 nm (Table 2), which suggested that the electron-withdrawing *o*-carborane is in conjugation with the backbone system; then the energy absorbed by the fluorene units is transferred to the *o*-carborane cluster and emitted in the orange region (Table 2). Furthermore, carborane-containing polymers **45a** and **45b** showed blue-shifted emission in the solid state compared to the solution state that was attributed to the forced aggregation of adjacent fluorene segments (Table 2). Contrary to poly(dihexylfluorene), annealing studies on **43** films showed a minimal increase in green emission after heating to 180 °C in air for 2 h. *o*-Carborane suppresses the green emission that commonly plagues blue-emitting polyfluorene systems. The fluorescence spectrum of **45a** in the solid-state displays a green emission centered at 520 nm that seems to occur by excimer formation due to aggregation. After annealing in air at 180 °C for 2 h, the films showed no shift in the emission wavelength but an increase in intensity, which is likely a result of increased aggregation from rearrangements above  $T_g$ .

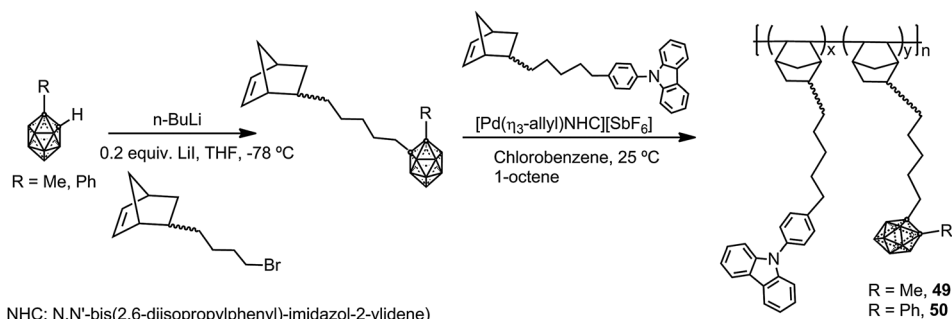
In parallel, two different polyfluorenes bearing pendant silylcarboranes **47** and **48** were prepared by homopolymerization

or copolymerization of the monomer **46** by microwave-assisted Yamamoto nickel-mediated aryl-aryl coupling reaction (Scheme 9).<sup>31</sup> The  $M_n$  was found to plateau at  $\sim 7000 \text{ g mol}^{-1}$  for all polymers obtained in the temperature range 10–150 °C. The emission spectra of the thin films of **47** before and after annealing for 3 h at 160 °C indicated that the fluorescence emission maximum was blue-shifted with respect to conventional fluorenes (Table 2), with a decrease in intensity when increasing carborane content. The presence of pendant carborane clusters elevates  $T_g$  and hinders chain packing, increasing stability and color purity, two essential properties of display materials.

Photoluminescent but no  $\pi$ -conjugated polynorbornene copolymers with pendant carbazoles and methyl- (**49**) or phenyl-*o*-carboranes (**50**) were synthesized as described in Scheme 10.<sup>32</sup> These copolymers possess high thermal stability and glass transition temperatures,  $T_{d5} > 410 \text{ °C}$  and  $T_g > 350 \text{ °C}$ , respectively. Due to the carbazole group, polymer **49** exhibits emission bands at around 351 nm and 366 nm, whereas polymer **49** that contains Ph-*o*-carborane shows quenching of the fluorescence as a result of the photoinduced CT process from the donor (carbazole) to the acceptor (Ph-*o*-carborane). Contrarily, when polymer **50** was treated with KOH/EtOH to produce the partial degradation of the cluster, the quenching process is blocked, and the material shows fluorescence emission.



Scheme 9 Microwave-assisted homopolymerization and copolymerization of monomer **46** to produce polymers **47** and **48**, respectively.

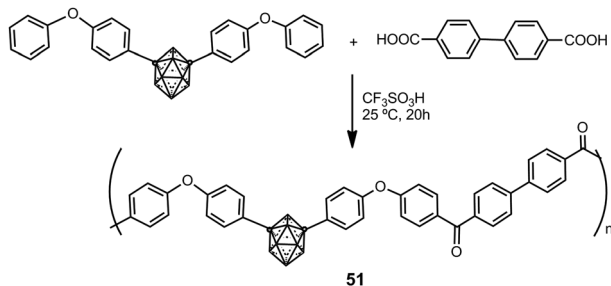


Scheme 10 Preparation of the polynorbornene copolymers **49** and **50**.



### III. Carborane-based polymers with other organic linkers

Hybrid organic–inorganic polyaryl(ether-ketone) containing aromatic rings and *o*- or *m*-carborane clusters in the main chain were synthesized using a typical superacid-promoted polycondensation reaction between bis(4-phenoxyphenyl) derivatives of *o*- or *m*-carborane and aromatic or aliphatic dicarboxylic acids.<sup>33</sup>

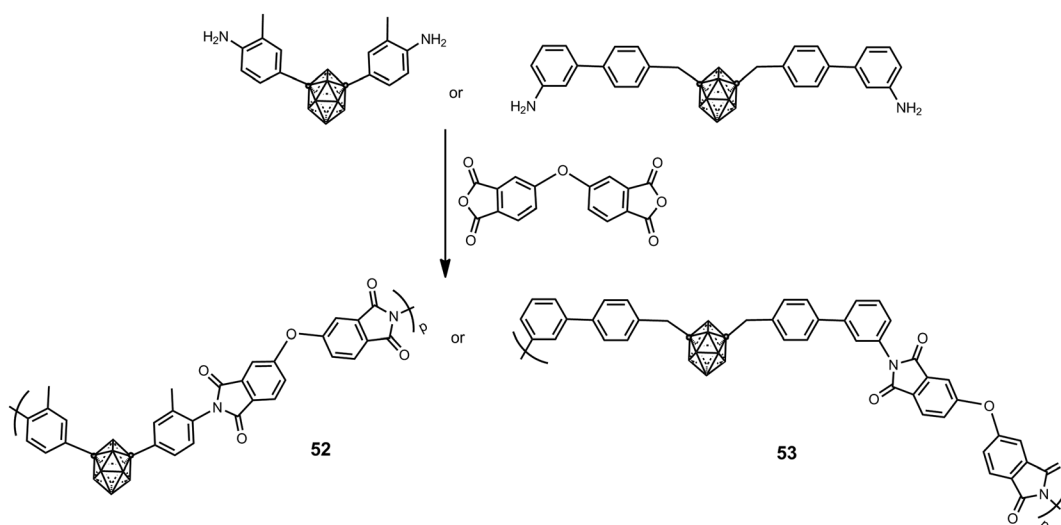


Scheme 11 Preparation of poly-aryl(ether-ketone)s containing *m*-carborane.

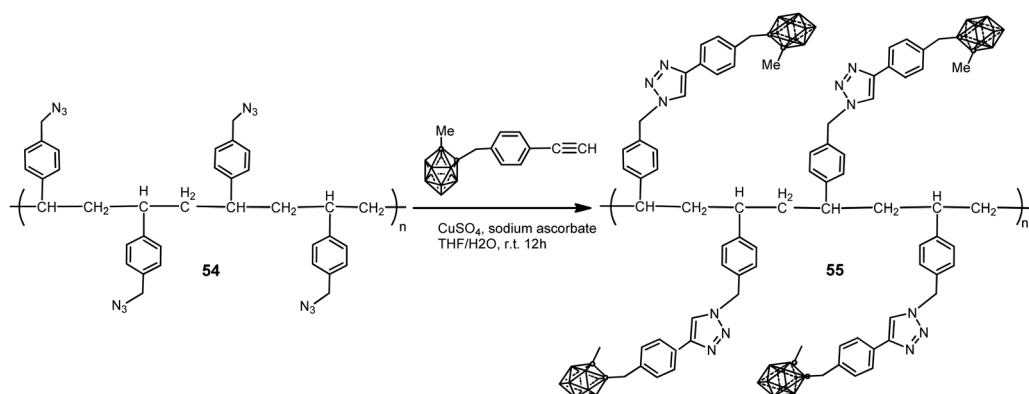
Scheme 11 displays the preparation of polymers **51** starting from a *m*-carborane derivative. Polymers were obtained in high molecular weights ( $M_w > 150\,000$ ). These materials are amorphous and readily soluble in organic solvents, to give solutions from which strong and transparent films may be obtained. These polymers showed very high mass-retention upon thermolysis: up to 93% and 97% under  $N_2$  or air, respectively.

Soluble *m*-carborane polyimide polymers such as **52** and **53**, which possess different types of structures, were prepared according to Scheme 12 in moderate molecular weight from 10 000 to 24 000  $g\ mol^{-1}$ .<sup>34</sup> These polyimides are non-crystalline materials; this is attributed to the bulkiness of the *m*-carborane cluster that disrupts intermolecular interactions and hinders regular and dense chain packing. The introduction of the *m*-carborane greatly increases their thermal stability, in which  $T_{d5}$  values exceed 600 °C in  $N_2$  and 100 °C in air.

A polystyrene polymer containing *o*-carborane components covalently linked to the side chain was prepared by the  $Cu^I$ -catalyzed Huisgen-type “click” reaction between the azidomethyl-appended polystyrene polymer **54** and the ethynyl-terminated carborane leading to polymer **55** (Scheme 13).<sup>35</sup>



Scheme 12 Preparation of polyimides bearing the *m*-carborane cluster.



Scheme 13 Synthesis of polymer **55** by “click” reaction.



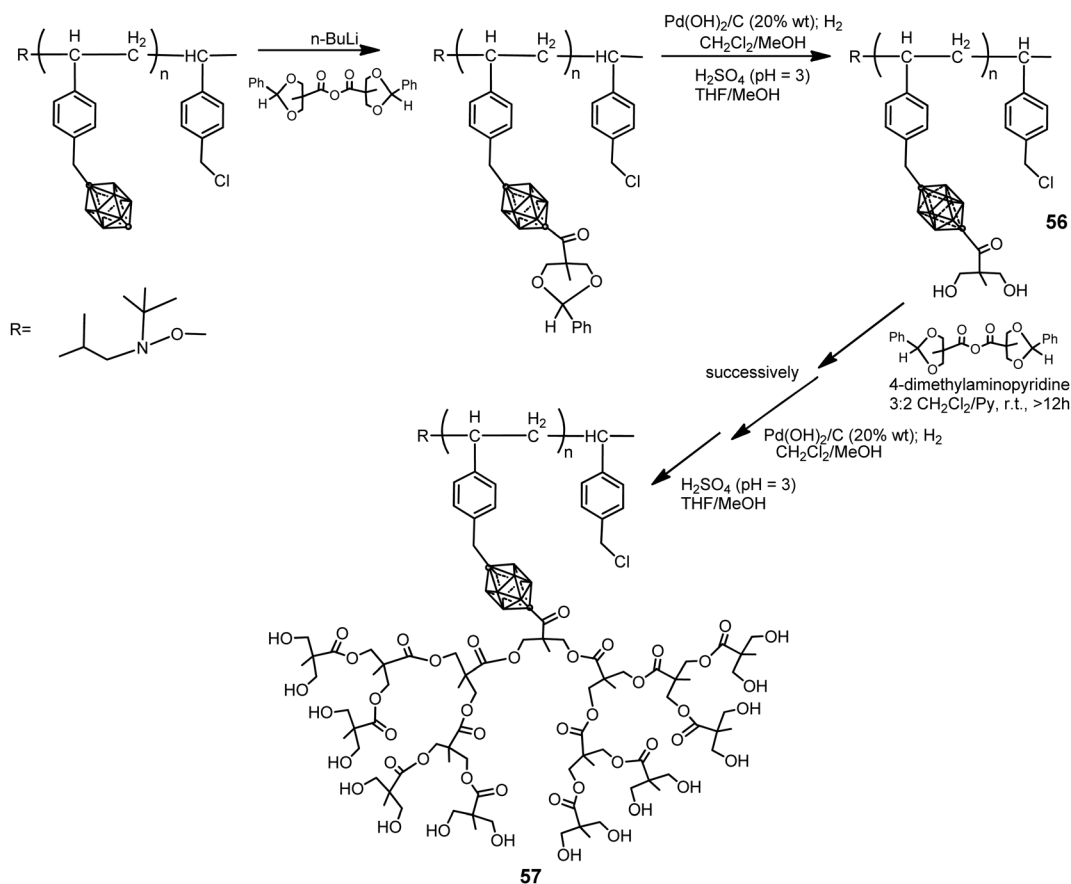


The carborane-appended styrenyl polymer has a polydispersity index (PDI) of 1.52 and good thermal robustness.

The *p*-carborane-containing polymer **56** was synthesized by following the procedure displayed in Scheme 14.<sup>36</sup> Polymers **56** were dendronized using a divergent approach to introduce aliphatic polyester dendrons (generation 1 to 4) grafted to the backbone of polymer branches to yield the dendronized polymer **57**. This approach afforded a maximum degree of dendronization of 70%. To increase the degree of dendronization, a first-generation macromonomer was polymerized using NMP to yield a fully functionalized first-generation dendronized polymer, which was then dendronized up to the fourth generation. Both approaches produced water-soluble dendronized

polymers (1 mg mL<sup>-1</sup> in pure water) with high molecular weights (in excess of 70 kDa), with potential biomedical applications, narrow molecular weight distributions and a polydispersity index (PDI) < 1.1.

Amphiphilic carborane-containing diblock copolymers represented by polymer **58** were synthesized from 1-OH(CH<sub>2</sub>)<sub>3</sub>-2-SiMe<sub>2</sub>*t*Bu-1,2-C<sub>2</sub>B<sub>10</sub>H<sub>10</sub> following the procedure described in Scheme 15.<sup>37</sup> The diblock copolymers were obtained by sequential addition of the silyl-protected oxonorborene imide carborane derivative and Boc-protected oxonorborene imide amine in different molar ratios. These copolymers were obtained with molecular weights ranging from 17 to 65 kg mol<sup>-1</sup> and high PDI from 1.09 to 1.15.



Scheme 14 Preparation and dendronization of polymer **56**.



Scheme 15 Formation of carborane-containing diblock copolymers.

## IV. Icosahedral boron cluster-containing silane and siloxane-polymers

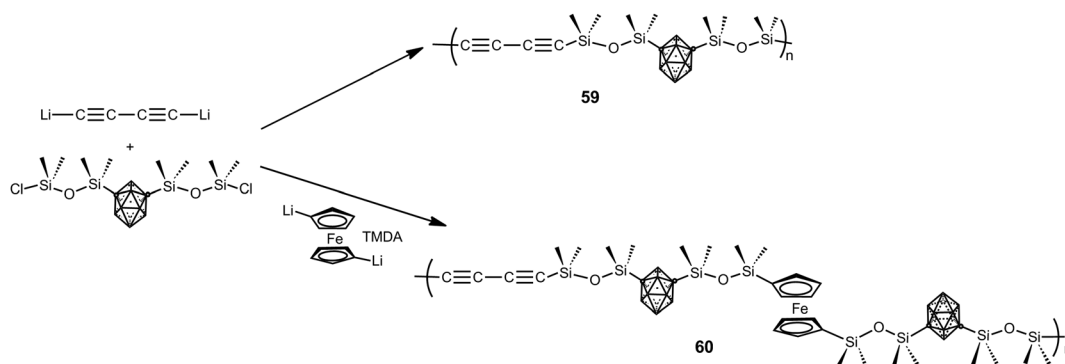
Besides the previous polymers, a large family of hybrid organic-inorganic polymers is formed by silane and siloxane-based polymers.<sup>4</sup> The report of the first siloxy-*m*-carborane polymers dates back to the 1960s with the development of commercial DEXSIL and UCARSIL polymers used as stationary phases for high-temperature gas chromatography compounds. In the 70s of the last century, Donald D. Stewart reported different methods to obtain linear high molecular weight D2-*m*-carborane siloxanes with molecular weights up to ( $>10^6$ ). The ultra-high molecular weight polymers exhibited improved thermal and mechanical properties as a result of increased chain entanglement of the polymer chains.<sup>4</sup>

Later, a series of carborane-siloxane-acetylene polymers with outstanding exceptional thermal and oxidative degradation properties were developed. Polymers **59** and **60** were synthesized from 1,7-(SiMe<sub>2</sub>OSiMe<sub>2</sub>Cl)<sub>2</sub>-1,7-C<sub>2</sub>B<sub>10</sub>H<sub>10</sub> following the procedure shown in Scheme 16. Thermal cross-linking of **59** produces a

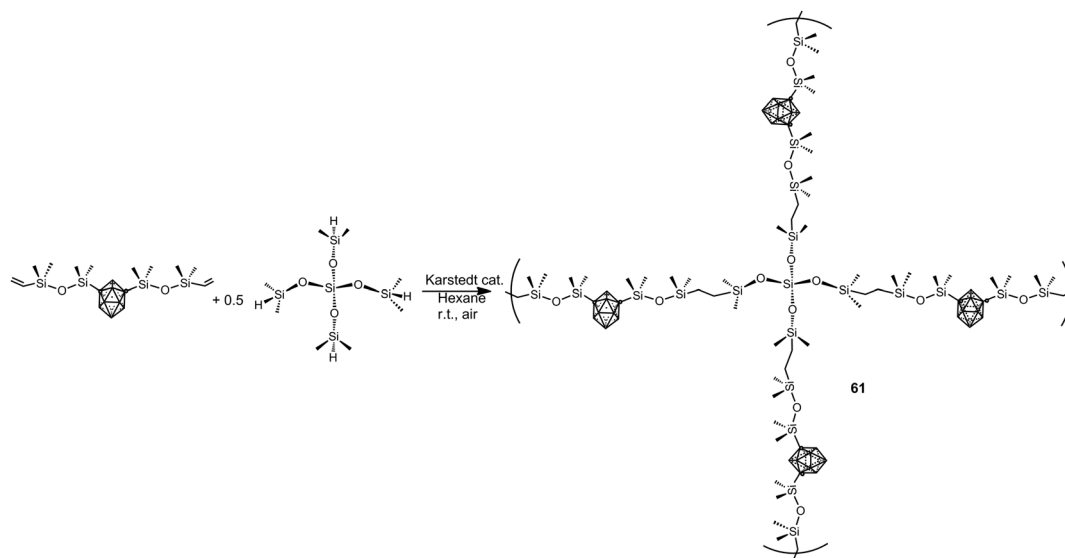
thermoset that gave a ceramic material in high yield after pyrolysis at 1000 °C. Polymer **60** exhibits high thermal stability, with weight retention of 78% at 1000 °C, when compared with other ferrocenyl-siloxane polymers.<sup>4</sup> To develop high temperature elastomers upon thermal curing, a set of *m*-carborane-trisiloxane-diacetylene copolymers were prepared varying acetylenic frequencies in the backbone, with trisiloxane:carborane:diacetylene molar ratios of 10:9:1, 5:4:1 and 3:2:1. Variation in the copolymer sequence caused noticeable differences in the calorimetric glass transitions for those in which the diacetylene group was most concentrated.<sup>38</sup>

More recently, elastomeric *m*-carborane-siloxane polymers **61** have been prepared *via* a rapid Karstedt-catalyzed hydrosilylation reaction using a branched siloxane crosslinker monomer (Scheme 17).<sup>39</sup> The elasticity of polymers can be modulated by careful choice of the crosslinkers. The obtained polymers show an oxidative stability up to 300 °C and their *T*<sub>d5</sub> are in the range 500–550 °C.

Poly(carborane-siloxane arylacetylene) polymers **62** and **63** were synthesized from the 1,7-(SiMe<sub>2</sub>OSiMe<sub>2</sub>Cl)<sub>2</sub>-1,7-C<sub>2</sub>B<sub>10</sub>H<sub>10</sub>



Scheme 16 Preparation of carborane-siloxane-acetylene polymers.



Scheme 17 Example of the preparation of *m*-carborane-siloxane polymers *via* Karstedt-catalyzed hydrosilylation reaction.





Scheme 18 Preparation of poly(carborane-siloxane arylacetylene) polymers **62** and **63**.

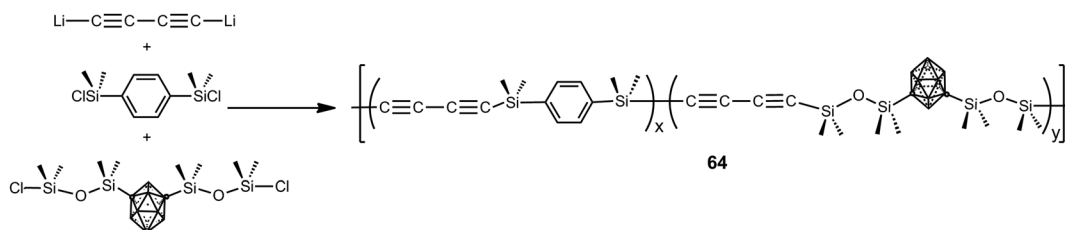
monomer and Grignard derivatives (Scheme 18).<sup>40</sup> Their thermal treatment results in a fully crosslinked thermoset by 500 °C as a consequence of cycloaddition reactions involving the acetylene and aryl functionalities and subsequent formation of bridging disilylmethylene entities. The developed polymers have exceptional thermo-oxidative properties similar to their diacetylene counterpart poly(carborane-siloxane-acetylene) and enhanced mechanical properties for the thermoset samples when compared to poly(siloxane-acetylene).

Polymers **64** were prepared by polycondensation reaction of 1,4-dilithiobutadiyne with 1,4-bis(dimethylsilyl)benzene and 1,7-(SiMe<sub>2</sub>OSiMe<sub>2</sub>Cl)<sub>2</sub>-1,7-C<sub>2</sub>B<sub>10</sub>H<sub>10</sub> by varying the molar ratios as follows: 100:0, 75:25, 50:50, 25:75 and 0:100 (Scheme 19).<sup>4</sup> These polymers were viscous liquids or low melting solids at room temperature and show good solubility in different solvents, such as THF, acetone, diethyl ether and chloroform. These polymers show good thermal stability giving high char yield (79–86%) when heated to 1000 °C under N<sub>2</sub>. Aging studies performed at elevated temperatures in air on a thermoset and a ceramic showed that these systems have excellent thermal and oxidative stability.

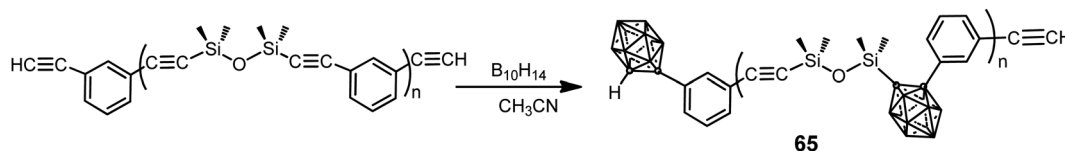
A series of poly(silylene-arylacetylene)s and poly(siloxane-arylacetylene)s with *o*-carborane in the backbone were prepared by the coupling reaction between the corresponding poly(silylene-arylacetylene) (PSA) or poly(siloxane-arylacetylene) (PSOA) and decaborane (B<sub>10</sub>H<sub>14</sub>) with different molar ratios (B<sub>10</sub>H<sub>14</sub>/PSOA: 0.6, 1.2, 1.8, 2.4) (Scheme 20).<sup>41</sup> The resulting

carboranyl-containing PSOA polymers **65** could be converted into a thermoset below 250 °C. The thermosets from carboranyl-containing PSA exhibit excellent thermal and thermo-oxidative stabilities with 91.5% residue yield in N<sub>2</sub> and 95.8% in air at 800 °C, whereas thermosets from polymer **65** exhibit oxidation-resistance with over 85% residue yields at 1000 °C in air.

The use of 1,7-(SiMe<sub>2</sub>OSiMe<sub>2</sub>Cl)<sub>2</sub>-1,7-C<sub>2</sub>B<sub>10</sub>H<sub>10</sub> as starting material in previous poly(carborane-siloxane-diacetylene) polymers **59–60** and **62–64** has limited their research due to the difficulties in obtaining it. This forced to synthesize other kinds of polymers such as poly(carborane-silane) (**66**), which was obtained by the procedure displayed in Scheme 21.<sup>4</sup> These polymers are viscous liquids at room temperature with a molecular weight distribution with a PDI of 1.67 and *M*<sub>n</sub> of 2853 g mol<sup>−1</sup>. Polymers **66** show very good solubility in common organic solvents (THF, diethyl ether, and acetone), offering good processability to fabricate composites. Thermoset exhibits excellent thermal and oxidative properties. The *T*<sub>d5</sub> is 762 °C and char yield is 94.2% at 800 °C in N<sub>2</sub>, whereas *T*<sub>d5</sub> is greater than 800 °C and char yield is 95.6%, at 800 °C in air. After pyrolysis, the char has no additional weight loss up to 800 °C in air. Therefore, polymer **66** offers better mechanical and thermal stability than poly(carborane-siloxane-diacetylene) polymers, making the former a suitable candidate as a matrix resin for advanced composites and as a precursor for ceramics, whereas the latter can be used as a high temperature elastomer.



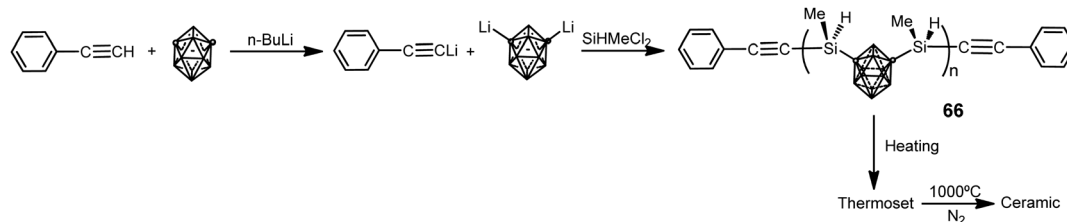
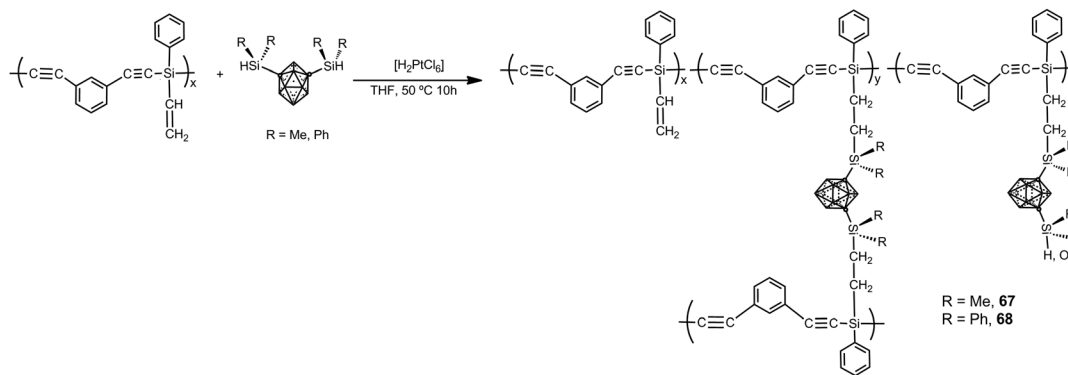
Scheme 19 Preparation of polymer **64**.



Scheme 20 Preparation of poly(siloxane-arylacetylene)s **65** from B<sub>10</sub>H<sub>14</sub>.





Scheme 21 Procedure for the preparation of poly(carboranesilane) **66**.Scheme 22 Preparation of polymers **67** and **68**.

Carborane–silane–acetylene polymers **67** and **68** have been prepared by hydrosilylation reaction of diethynylbenzene-silene polymers and 1,7-[HSi(Me)<sub>2</sub>]<sub>2</sub>-1,7-C<sub>2</sub>B<sub>10</sub>H<sub>10</sub> or 1,7-[HSi(Ph)<sub>2</sub>]<sub>2</sub>-1,7-C<sub>2</sub>B<sub>10</sub>H<sub>10</sub> (Scheme 22). Polymers possess a weight-average molecular weight of  $M_w = 21\,600$ .<sup>42</sup> In air, no weight loss up to 600 °C occurs with a ceramic yield of up to 95% at 800 °C, whereas under N<sub>2</sub> the polymer showed high performance with ceramic yields more than 90% at 800 °C. These polymers exhibit high mechanical and thermal stability as well as flame retardant properties. Additionally, the polymer possesses a relatively high strength with a flexural modulus of 1.86 GPa and 0.95 GPa at room temperature and 250 °C, respectively.

## V. Coordination polymers incorporating icosahedral boron clusters

Coordination polymers (CP) are infinite multidimensional (1D linear or twisted chains, 2D squares and polygons and 3D cubes and polyhedra) materials with highly ordered structures. These structures are highly conditioned by the nature of multifunctional ligands and the coordination requirements of the metallic centres or the counter-ions. A slight modification in any of these factors can lead to new structures and consequently new properties. The presence of metal–ligand association can lead to suitable materials with particular usefulness or applicability; the metal can provide redox and magnetic properties among others and the appropriate ligand may determine the functionality of the material. On the other hand, polynuclear metal complexes attract great interest owing to their relevance to many important naturally occurring

processes. The cooperative action of closely coupled dinuclear or multinuclear centers is required for several enzymes to carry out their biological functions for example in the photosystem II. In this sense, the further design and construction of new supramolecular assemblies as models of the oxygen-evolving centre (OEC) can facilitate the understanding of the role of water molecules in the catalytic process of water splitting.

Borane and carborane clusters are ligands of great interest in supramolecular chemistry because of their particular properties,<sup>4</sup> which may induce unconventional properties in the supramolecular structures in which they are inserted. Even though boron clusters are considered as weak coordinating compounds, it has been demonstrated that they can form supramolecular polymeric structures not only due to the bridging of polymetallic centers by various non-boron ligands, but also *via* the so-called halogen or dihydrogen bonding of polyhedral clusters. The literature has accepted the use of the term “coordination polymer” where B–H...M interactions are the primary interactions in the polymeric structures.

This section of the review summarizes 1D-coordination polymer derivatives of icosahedral anionic *closo* [CB<sub>11</sub>H<sub>12</sub>]<sup>−</sup> and *nido* [C<sub>2</sub>B<sub>10</sub>H<sub>12</sub>]<sup>2−</sup> clusters, with special emphasis on the polymeric structures of metallaboranes and carboranes of main group metals, d- and f-block elements. During the writing of this paper, C. E. Housecroft published a review on carborane coordination polymers with transition metals;<sup>43</sup> therefore in this section we will only supplement this review with several new 1D-polymeric structures.

### 1. Polymers with main group metals

Neutral *closo* *o*-, *m*- and *p* carboranes are reduced by Group 1 metals. This reaction always results in the complete cleavage of the cage C<sub>c</sub>–C<sub>c</sub> bond, leading to the formation of “carbons-apart”



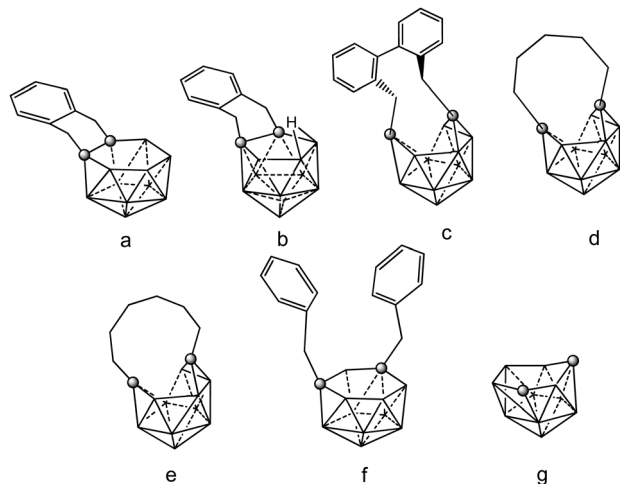


**Chart 7** View of the different positional 12 vertex *nido* carboranyl ligands involved in the coordination polymers (69)–(75). Vertices correspond to B–H while the circles to the C<sub>c</sub> atom.

*nido* [R<sub>2</sub>C<sub>2</sub>B<sub>10</sub>H<sub>10</sub>]<sup>2–</sup> isomers. Chart 7 displays the different positional isomers of 12 vertices *nido* carboranyl ligands that are involved in these coordination polymers. As a consequence of their high stability, these clusters are very useful synthons for the production of numerous metallocarboranes of s-, p-, d- and f-elements. To force the two cage carbon atoms of the starting *closo o*-carborane to remain adjacent, “carbons-adjacent”, during the reduction process, the most effective way is introducing a short linkage, C<sub>6</sub>H<sub>4</sub>(CH<sub>2</sub>)<sub>2</sub> or (CH<sub>2</sub>)<sub>3</sub>, between the two cage carbon atoms of the icosahedral *closo o*-carborane cluster.<sup>4</sup>

Polymeric structures of Group 1 salts have been obtained during the reduction of the corresponding *closo*-carboranes 1,2-Ar(CH<sub>2</sub>)<sub>2</sub>-1,2-C<sub>2</sub>B<sub>10</sub>H<sub>10</sub><sup>44</sup> (Ar = *o*-C<sub>6</sub>H<sub>4</sub>, 1,8-C<sub>10</sub>H<sub>6</sub>, 1,1'-C<sub>6</sub>H<sub>4</sub>) and 1,2-R-1,2-C<sub>2</sub>B<sub>10</sub>H<sub>10</sub>,<sup>45</sup> R = (CH<sub>2</sub>)<sub>5</sub>, (CH<sub>2</sub>)<sub>6</sub>, with excess of Na,

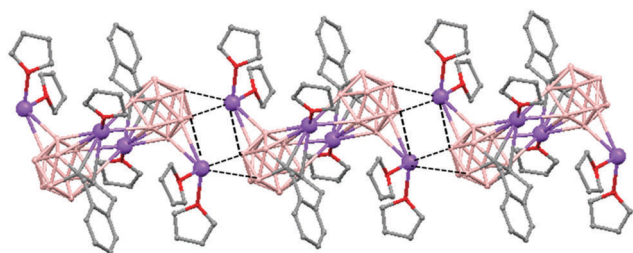


**Fig. 12** 1D-polymer chain of (69). H atoms omitted for clarity.

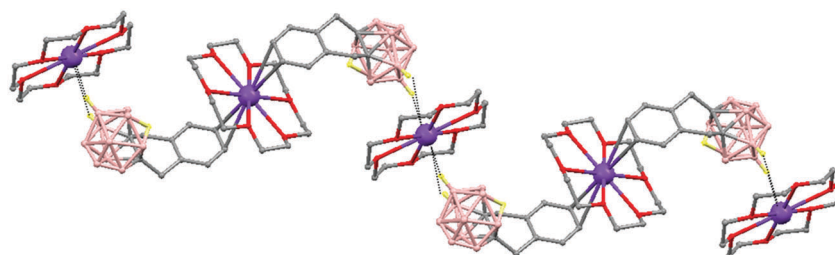


**Fig. 13** Molecular structure of (70). Some H atoms omitted for clarity.

K or Li metal in THF. The Group 1 metal polymers [{μ-1,2-[*o*-C<sub>6</sub>H<sub>4</sub>(CH<sub>2</sub>)<sub>2</sub>]-1,2-C<sub>2</sub>B<sub>10</sub>H<sub>10</sub>]<sub>2</sub>{Na<sub>4</sub>(THF)<sub>6</sub>}]<sub>n</sub> (69), and [{μ-1,2-[*o*-C<sub>6</sub>H<sub>4</sub>(CH<sub>2</sub>)<sub>2</sub>]-1,2-C<sub>2</sub>B<sub>10</sub>H<sub>11</sub>}{K(18-crown-6)<sub>2</sub>}]<sub>n</sub> (70) maintain the two carbon atoms adjacent after the reduction process.<sup>44</sup> However, [{μ-1,4-[1,1'-(C<sub>6</sub>H<sub>4</sub>)<sub>2</sub>-2,2'-(CH<sub>2</sub>)<sub>2</sub>]-1,4-C<sub>2</sub>B<sub>10</sub>H<sub>10</sub>}]Na<sub>2</sub>(THF)<sub>3</sub>]<sub>n</sub> (71),<sup>44</sup> [{1,3-(CH<sub>2</sub>)<sub>5</sub>-1,3-C<sub>2</sub>B<sub>10</sub>H<sub>10</sub>}]Na<sub>2</sub>(THF)<sub>4</sub>]<sub>n</sub> (72) and [{1,4-(CH<sub>2</sub>)<sub>6</sub>-1,4-C<sub>2</sub>B<sub>10</sub>H<sub>10</sub>}]Na<sub>2</sub>(THF)<sub>4</sub>]<sub>n</sub> (73) polymers<sup>45</sup> present “carbons-apart” 12 vertex *nido*-carborane ligands as a result of the complete cleavage of the C<sub>c</sub>–C<sub>c</sub> bond. The <sup>1</sup>H-, <sup>13</sup>C- and <sup>11</sup>B-NMR spectra of the polymeric compounds show the presence of methylene protons at the bridges in the range of δ 4.86–2.50 ppm and also support the corresponding ratio of THF molecules per carboranyl for all compounds. In addition, their solid state IR spectra display bands in the range 2300–2500 cm<sup>–1</sup> characteristic of B–H...M interactions.

The polymeric structure of all complexes (69)–(73) was confirmed by single-crystal X-ray analysis. All compounds adopt a polymeric arrangement in which the metal atom (Na or K) and the 12 vertices *nido*-carborane ligand serve as alternating linkages to give a zigzag infinite chain that is maintained in one dimension throughout the lattice. In the case of (69)<sup>44</sup> (Fig. 12) each asymmetric unit consists of two [{μ-1,2-[*o*-C<sub>6</sub>H<sub>4</sub>(CH<sub>2</sub>)<sub>2</sub>]-1,2-C<sub>2</sub>B<sub>10</sub>H<sub>10</sub>}]Na<sub>2</sub>(THF)<sub>3</sub>] structural motifs that are related to each other by an inversion center. One Na<sup>+</sup> is η<sup>6</sup>-bound to the open six-membered C<sub>2</sub>B<sub>4</sub> face and coordinated to one THF molecule and one neighbouring ‘carbons-adjacent’ *nido*-carborane via two B–H...Na bonds. The second Na<sup>+</sup> is bonded to a trigonal B<sub>3</sub> face through three B–H...Na bonds and to the neighboring ‘carbons-adjacent’ *nido*-carborane via two B–H...Na bonds and coordinated to two THF molecules. The average Na(1)–cage atom and Na(2)...B(H) distances are of 2.854(4) and 3.026(4) Å, respectively.

The most significant part of the structure of polymer (70)<sup>44</sup> (Fig. 13) is the monoanion [R<sub>2</sub>C<sub>2</sub>B<sub>10</sub>H<sub>11</sub>]<sup>–</sup>, which was first observed experimentally. This ligand possesses two pentagonal belts: a C<sub>2</sub>B<sub>3</sub> that is partially capped by one μ<sub>3</sub>-H atom (Chart 7b) and one B<sub>5</sub> that is capped by the remaining two boron atoms.

Polymer (71)<sup>44</sup> (Fig. 14) shows the novel [*nido*-μ-1,4-R<sub>2</sub>C<sub>2</sub>B<sub>10</sub>H<sub>10</sub>]<sup>2–</sup> dianion (Chart 7c), which has a basket structure with a highly distorted six-membered C<sub>2</sub>B<sub>4</sub> ring. The average C<sub>c</sub>–C–C<sub>aryl</sub> angle of 109.7(2)° and the dihedral angle between the two aromatic rings of 68.9° in 71 are much smaller than in its parent *closo* μ-1,2-[1,1'-(C<sub>6</sub>H<sub>4</sub>)<sub>2</sub>-2,2'-(CH<sub>2</sub>)<sub>2</sub>]-1,2-C<sub>2</sub>B<sub>10</sub>H<sub>10</sub> molecule, 117.8(3)° and 66.1°, respectively.

On the other hand, polymers 72 and 73 show a similar zigzag carborane–Na–carborane–Na infinite chain but a different



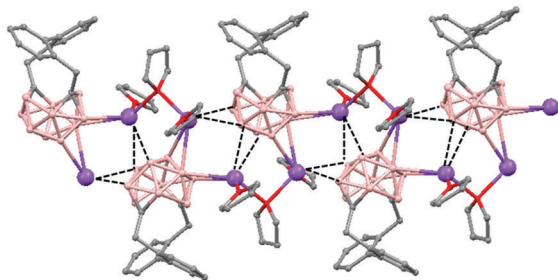


Fig. 14 Part of a 1D-chain in (71). H atoms omitted for clarity.

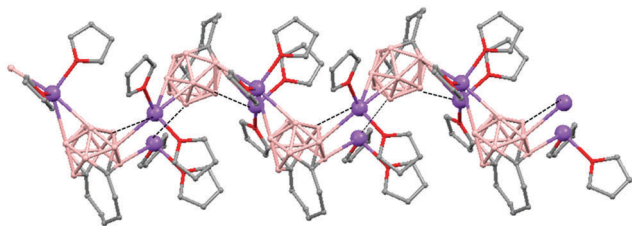


Fig. 15 Infinite polymer chain of (72). H omitted by clarity.

dianionic *nido*-carborane cage (Chart 7d and e).<sup>45</sup> The [*nido*-1,3-(CH<sub>2</sub>)<sub>5</sub>-1,3-C<sub>2</sub>B<sub>10</sub>H<sub>10</sub>]<sup>2-</sup> ligand in polymer 72 (Fig. 15) represents a new member of the 12-vertex *nido* cluster family, in which two connectivities, C<sub>c</sub>-C<sub>c</sub> and C<sub>c</sub>-B(3), are broken during the reductive process leading to the formation of a highly distorted five-member C<sub>2</sub>B<sub>3</sub> face with an elongated C(1)-B(3) bond (Chart 7d). In polymer [(1,4-(CH<sub>2</sub>)<sub>6</sub>-1,4-C<sub>2</sub>B<sub>10</sub>H<sub>10</sub>){Na<sub>2</sub>(THF)<sub>4</sub>}]<sub>n</sub> (73) as the linkage size increases by one methylene unit, the C(1)-B(3) distance is forced to be further separated, generating a highly distorted six-membered C<sub>2</sub>B<sub>4</sub> face (Chart 7e). The structural parameters of the *nido*-carborane cage in 73 are close to those observed in polymer 71.<sup>44</sup> These data suggest that the overall ring forces of the (CH<sub>2</sub>)<sub>6</sub> and 1,1'-(C<sub>6</sub>H<sub>4</sub>)<sub>2</sub>-2,2'-(CH<sub>2</sub>)<sub>2</sub> links acting on the cage are similar, although the rigidity of the bridges is quite different. These results show that although both the bridge length and the rigidity of C,C'-linked *o*-carboranes have significant effects on the formation of carborane anions, the former plays a more important role than the latter in controlling the relative positions of the two cage carbon atoms during the reductive process.<sup>45</sup>

The first structurally characterized example of a metallocarborane of K<sup>+</sup> corresponds to the polymer [*closo-exo*-{(C<sub>6</sub>H<sub>5</sub>CH<sub>2</sub>)<sub>2</sub>-C<sub>2</sub>B<sub>10</sub>H<sub>10</sub>}[K<sub>2</sub>(THF)<sub>2</sub>(O<sub>2</sub>C<sub>4</sub>H<sub>8</sub>)0.5}]<sub>n</sub> (74)<sup>46</sup> that adopts a structure in which the dioxane and the potassium ion serve as alternating bridging groups to give a zigzag chain (Fig. 16). One K<sup>+</sup> ion is η<sup>6</sup>-bonded to the hexagonal C<sub>2</sub>B<sub>4</sub> face of the cage forming a 13-vertex metallocarborane structural motif (Chart 7f) that is also coordinated to one oxygen atom of the bridging dioxane molecule. The other K<sup>+</sup> ion is bonded to two trigonal B<sub>3</sub> faces through two sets of three unequal B-H...K bonds from two neighboring carborane cages; its coordinating sphere is completed by two THF molecules.

In general, metallocarboranes of the heavier Group 2 metals are fewer in number; the only structurally characterized example

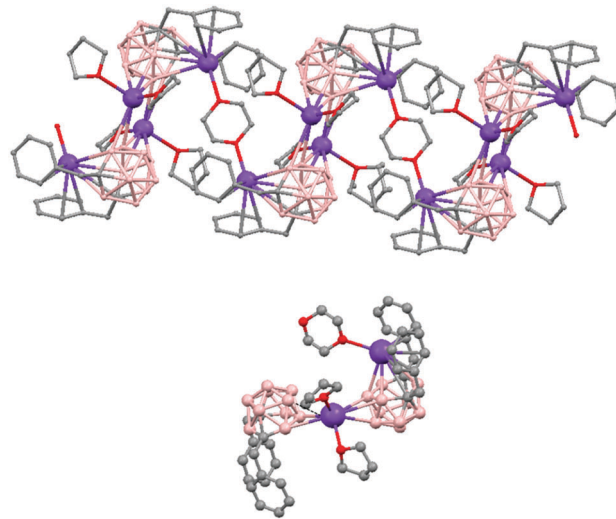


Fig. 16 Infinite polymeric chain of (74) together with a closer view of the coordination environment in polymer (74) (H omitted for clarity).

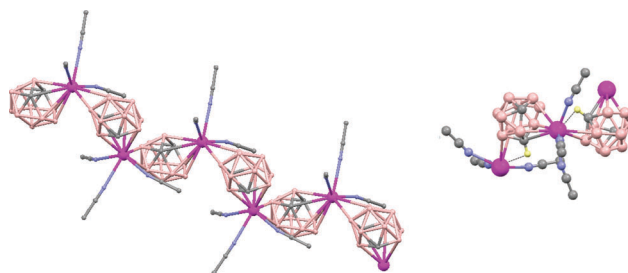


Fig. 17 Infinite polymer chain of (75). (H atoms omitted by clarity) with a magnified view to visualize the metal to carboranyl ligand interactions.

of a polymeric metallocarborane of Group 2 salts corresponds to the compound [*closo*-1,1,1-(MeCN)<sub>3</sub>-1,2,4-Sr(C<sub>2</sub>B<sub>10</sub>H<sub>12</sub>)]<sub>n</sub> (75) (Fig. 17).<sup>4</sup> The structure shows a spiral-chain whose units are linked by inter-cage Sr-H-B and Sr-H-C. Each carborane fragment (Chart 7g) serves as a ligand to two Sr atoms, bonded to one through an open hexagonal face and to the other *via* upper- and lower- belt E-H...M (E = B or C) interactions. The coordination geometry about each Sr is completed by three CH<sub>3</sub>CN ligands. It is noteworthy that one of the C-H vertices of each carborane fragment interacts with the Sr. A more detailed view of the metal to the carborane interaction can be seen in Fig. 17.

Polymeric structures of the heavier Group 14 elements, Sn and Pb, with carborane were prepared by chloride ion abstraction from [SnEt<sub>3</sub>]Cl and [PbEt<sub>3</sub>]Cl, respectively, using the halogenated carborane anion [CB<sub>11</sub>H<sub>6</sub>Br<sub>6</sub>]<sup>-</sup>.<sup>47</sup> Crystal structures [Et<sub>3</sub>E(CB<sub>11</sub>H<sub>6</sub>Br<sub>6</sub>)]<sub>n</sub> (E = Sn (76) or Pb (77)) adopt five-coordinate trigonal-bipyramidal geometries. The carborane anions are bridging axial ligands connecting trigonal [EEt<sub>3</sub>]<sup>+</sup> cation-like moieties in the polymeric chain structures, through Br atoms of the [CB<sub>11</sub>H<sub>6</sub>Br<sub>6</sub>]<sup>-</sup> unit (Fig. 18).

## 2. Polymers with d-block elements.

The treatment of [NMe<sub>4</sub>][1,1'-(PPh<sub>2</sub>)<sub>2</sub>-3,3'-Co(1,2-C<sub>2</sub>B<sub>9</sub>H<sub>10</sub>)<sub>2</sub>] with one equivalent of AgClO<sub>4</sub> in ethanol/acetone leads to a





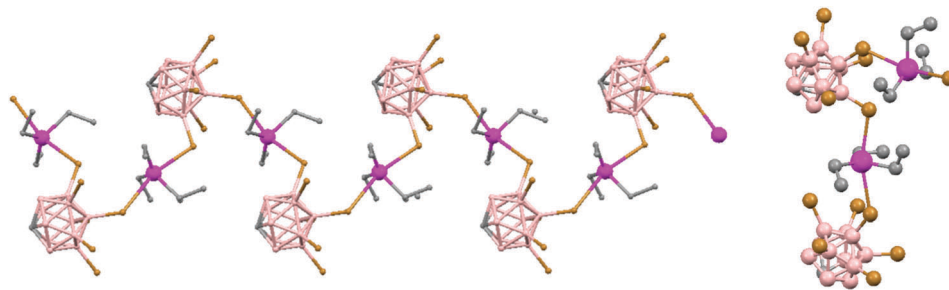


Fig. 18 Infinite polymer chain of (76) together with a view of the coordinating sphere around every K atom in (77). H atoms omitted for clarity.

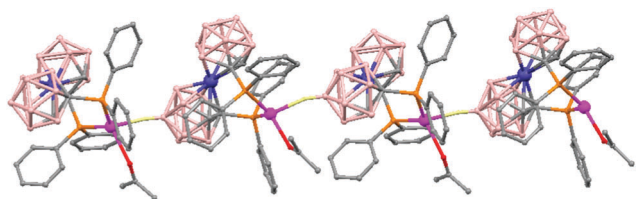


Fig. 19 Polymeric structure of (78), showing how the repetitive units are connected to neighbouring molecules. H atoms omitted for clarity with the exception of B–H...Ag interactions.

1D-coordination polymer  $[\text{Ag}\{1,1'-(\text{PPh}_2)_2-3,3'-\text{Co}(1,2-\text{C}_2\text{B}_9\text{H}_{10})_2\}(\text{OCMe}_2)]_n$  (78) (Fig. 19).<sup>48</sup> The silver cation is tetrahedrally coordinated by two P atoms from the carborane, one O atom from the acetone ligand and one neighboring *closo*-carborane *via* one B–H...Ag. The H...Ag distance of 2.17 Å is shorter than distances observed in other silver polymers containing the (1) anion.<sup>43</sup>

The incorporation of carborane clusters as linkers in coordination polymers can be realized by introducing the metal-binding group directly bonded to the cage. Carboranycarboxylate ligands have been used to introduce  $\text{C}_2\text{B}_{10}$ -cages into the backbone of 1D coordination polymers. The reaction of two different carboranycarboxylate ligands, 1-R-2- $\text{CO}_2\text{H}$ -1,2-*closo*- $\text{C}_2\text{B}_{10}\text{H}_{10}$  (R = CH<sub>3</sub>, H) with  $\text{MnCO}_3$  in water leads to the polymeric compounds  $[\text{Mn}(\mu\text{-H}_2\text{O})(\mu\text{-1-CH}_3\text{-2-CO}_2\text{-1,2-}i\text{closo-C}_2\text{B}_{10}\text{H}_{10})_2]_n \cdot (\text{H}_2\text{O})_n$  (79)<sup>49</sup> or  $[\text{Mn}(\text{H}_2\text{O})(\mu\text{-1-CO}_2\text{-1,2-}i\text{closo-C}_2\text{B}_{10}\text{H}_{11})_2]_n \cdot 2\text{H}_2\text{O}$  (80),<sup>50</sup> respectively. X-ray analysis (Fig. 20a and b) revealed substantial differences between both compounds attributed to the existence of different substituents, –CH<sub>3</sub> or –H, on one of the C<sub>c</sub> of the carboranycarboxylate ligand. While a six-coordinated  $\text{Mn}^{\text{II}}$

compound with water molecules bridging each two  $\text{Mn}^{\text{II}}$  centers was observed in (79), a square pyramidal geometry around each  $\text{Mn}^{\text{II}}$  ion with terminal water molecules coordinated to each  $\text{Mn}^{\text{II}}$  center was found (80). The structures of these polymers display an unusual feature among the 1D oligomer  $\text{Mn}^{\text{II}}$  complexes with a nuclearity higher than two, that is, the existence of water molecules bridging two Mn centers or the existence of terminal water molecules depends on the carboranycarboxylate ligand used.

The packing structure of polymer (79) displays polymeric chiral chains with two different conformations (*Δ* and *Λ*) due to the orientation of the CH<sub>3</sub> groups from the carboranycarboxylate ligands (Fig. 21). The orientation of the CH<sub>3</sub> groups is the same within a chain and opposite to the CH<sub>3</sub> groups from a different chain. However, the polymeric chiral chains displayed in (79) are not observed in (80).

The polymeric nature of both compounds can be easily fragmented by coordinating solvents, *e.g.* diethyl ether, generating oligomer species. Moreover, the reactivity of polymer (79) with Lewis bases, such as 2,2'-bipyrimidine, leads to the formation of a new hybrid polymer  $[\text{Mn}(1\text{-CH}_3\text{-2-CO}_2\text{-1,2-}i\text{closo-C}_2\text{B}_{10}\text{H}_{10})_2(\text{bpm})]_n$  (81) (Fig. 22). Magnetic measurements show weak antiferromagnetic interactions between the Mn atoms in all cases.

### 3. Polymers with f-block elements

The reaction of  $[\text{Me}_2\text{Si}(\text{C}_9\text{H}_5\text{CH}_2\text{H}_2\text{OMe})(\text{C}_2\text{B}_{10}\text{H}_{10})]\text{Li}_2(\text{OEt}_2)_2$  with an equimolar amount of  $\text{SmI}_2$  in THF results in the isolation of the polymer  $\{[\{\eta^5\text{-}\sigma\text{-Me}_2\text{Si}(\text{C}_9\text{H}_5\text{CH}_2\text{CH}_2\text{OMe})(\text{C}_2\text{B}_{10}\text{H}_{10})\}_2\text{Sm}\}\text{-}\{\text{Li}(\text{THF})\}\}_n$  (82).<sup>51</sup> Compound (82) is a coordination polymer with Li(THF) as a linkage connecting two anionic  $[\{\{\eta^5\text{-}\sigma\text{-Me}_2\text{Si}(\text{C}_9\text{H}_5\text{CH}_2\text{CH}_2\text{OMe})(\text{C}_2\text{B}_{10}\text{H}_{10})\}_2\text{Sm}\}]^-$  fragments *via* the

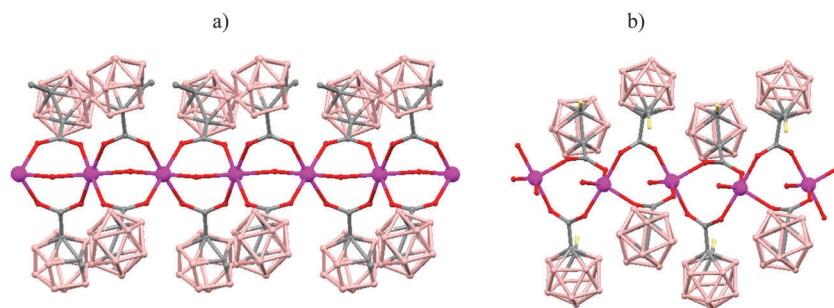


Fig. 20 Structure of polymers (79) and (80) showing the monodimensional arrangement. H atoms and water solvate omitted with the exception of the H substituent in (80).







Fig. 21 X-ray structure of (79) showing different conformations for the polymeric chains. (Reproduced from ref. 47 with permission from the Royal Society of Chemistry).



Fig. 22 Infinite polymer chain of the hybrid  $[\text{Mn}(\text{1-CH}_3\text{-2-CO}_2\text{-1,2-closo-C}_2\text{B}_{10}\text{H}_{10})_2(\text{bpm})]_n$  (81) (H atoms omitted for clarity).



Fig. 23 Infinite polymer chain of (82). H atoms omitted for clarity.

tethered oxygen atoms (Fig. 23). The formation of (82) results from the  $\text{Sm}(\text{II})$  electron transfer to the cluster. It may be suggested that the reaction of  $\text{SmI}_2(\text{THF})_x$  with  $[\text{Me}_2\text{Si}(\text{C}_9\text{H}_5\text{C}_2\text{H}_2\text{OMe})(\text{C}_2\text{B}_{10}\text{H}_{10})]\text{Li}_2(\text{OEt}_2)_2$  gives the first intermediate  $[\eta^5:\eta^1:\sigma\text{-Me}_2\text{Si}(\text{C}_9\text{H}_5\text{CH}_2\text{-CH}_2\text{OMe})(\text{C}_2\text{B}_{10}\text{H}_{10})]\text{Sm}^{\text{II}}$ , followed by intermolecular electron transfer and then ligand redistribution to afford polymer (82).

The reaction of  $\text{EuI}_2(\text{THF})_2$  with equimolar amounts of  $\text{Na}_2\text{-[nido-C}_2\text{B}_{10}\text{H}_{12}]$  in THF results in the isolation of half-sandwich lanthanacarborane  $[(\eta^6\text{-C}_2\text{B}_{10}\text{H}_{12})\text{Eu}(\text{THF})_3]_n$  that after recrystallization from MeCN/Et<sub>2</sub>O gives a MeCN coordinated species  $[(\eta^6\text{-C}_2\text{B}_{10}\text{H}_{12})\text{Eu}(\text{MeCN})_3]_n$  (83) (Fig. 24).<sup>52</sup> Single-crystal X-ray analyses show a spiral chain where each carborane moiety serves as a ligand for two europium atoms, and each  $\text{Eu}^{2+}$  ion is  $\eta^6$ -bonded to one  $\text{C}_2\text{B}_{10}\text{H}_{12}^{2-}$  ligand and  $\sigma$ -bonded to three MeCN molecules and two E–H (E = /cage B and C atoms) bonds from the neighboring carboranyl ligand in a highly distorted octahedral



Fig. 24 Infinite polymer chain of (83) (H atoms omitted for clarity).

geometry. The fragment  $\text{C}_2\text{B}_{10}$  in this compound can be compared with the previously described Sr metallocarborane polymer (75).

The reaction of  $\text{Me}_2\text{Si}(\text{C}_9\text{H}_7)(\text{C}_2\text{B}_{10}\text{H}_{11})$  with excess of NaH followed by Na metal afforded  $[\{\text{Me}_2\text{Si}(\text{C}_9\text{H}_7)(\text{C}_2\text{B}_{10}\text{H}_{11})\}[\text{Na}_3(\text{THF})_n]]$  that reacts with  $\text{ErCl}_3$  in THF leading to  $[\{\eta^5:\eta^6\text{-Me}_2\text{Si}(\text{C}_9\text{H}_6)(\text{C}_2\text{B}_{10}\text{H}_{11})\}\text{Er}(\text{THF})(\mu\text{-Cl})\text{Na}(\text{THF})_2\}]_n$  (84) (Fig. 25) after recrystallization from toluene/THF. This complex shows a polymeric chain where the  $\text{Er}^{3+}$  ion is  $\eta^5$ -bound to the indenyl group,  $\eta^6$ -bound to the hexagonal  $\text{C}_2\text{B}_4$  face of the *nido*-carborane cage,  $\sigma$ -bound to one bridging chlorine atom and coordinated to one THF molecule in a distorted-tetrahedral arrangement. The cation  $[\text{Na}(\text{THF})_2]^+$  acts as a linkage to connect two  $[\{\eta^5:\eta^6\text{-Me}_2\text{Si}(\text{C}_9\text{H}_6)(\text{C}_2\text{B}_{10}\text{H}_{11})\}\text{Er}(\text{THF})(\mu\text{-Cl})\}]^-$  fragments.

*closo* 1,2- $\text{C}_2\text{B}_{10}\text{H}_{12}$  can undergo four-electron reduction with excess alkali metals in the presence of f-block lanthanide metal halides to form an *arachno*  $[\text{C}_2\text{B}_{10}\text{H}_{12}]^{4-}$  tetraanion. This 12 vertex *arachno* cluster is capable of being  $\eta^7$ -bound to metal ions leading to 13-vertex *closo*-metallacarboranes, which can be obtained also through the *nido*-carborane lanthanide metals. Chart 8 shows different 12 vertex *arachno* carboranyl ligands involved in the coordination polymers (85)–(91).

The reaction of  $[\{\eta^5\text{-Me}_2\text{C}(\text{C}_5\text{H}_4)(\text{C}_2\text{B}_{10}\text{H}_{11})\}\{\text{ErCl}_2(\text{THF})_3\}]$  or  $[\{\eta^5:\eta^6\text{-Me}_2\text{C}(\text{C}_5\text{H}_4)(\text{C}_2\text{B}_{10}\text{H}_{11})\}\{\text{Er}(\text{THF})_2\}]$  with excess Na metal in THF at room temperature affords the same  $[\{\eta^5:\eta^7\text{-Me}_2\text{C}(\text{C}_5\text{H}_4)(\text{C}_2\text{B}_{10}\text{H}_{11})\}\text{Er}\}_2\{\text{Na}_4(\text{THF})_9\}]_n$  (85) compound.<sup>54</sup> The polymeric nature of (85) confirmed by X-ray diffraction indicates that each asymmetrical unit contains two  $[\eta^5:\eta^7\text{-Me}_2\text{C}(\text{C}_5\text{H}_4)(\text{C}_2\text{B}_{10}\text{H}_{11})\text{Er}]^{2-}$  structural motifs that are connected by three Na atoms through several B–H...Na three-center-two-electron bonds (3c–2e). The asymmetrical units are linked to each other *via* B–H...Er bonds to form a polymeric chain. Each metal ion is  $\eta^7$ -bound to the *arachno*-carboranyl ligand (Chart 8a),  $\eta^5$ -bound to the cyclopentadienyl and  $\sigma$ -bound to two B–H bonds from the neighboring *arachno*-carboranyl unit in a distorted tetrahedral arrangement.



Fig. 25 A portion of infinite polymer chain of (84) (H atoms omitted for clarity).



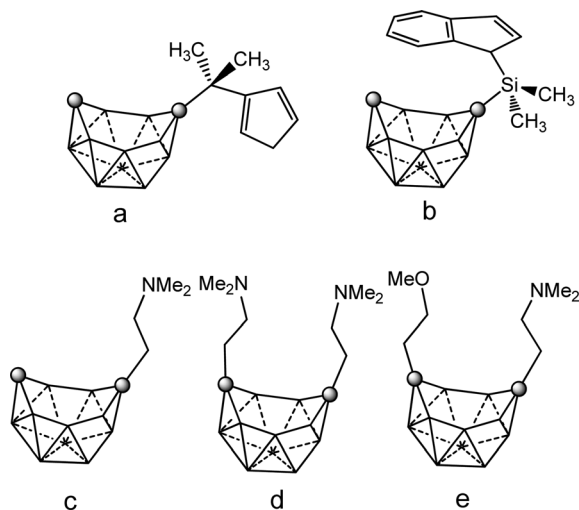


**Chart 8** View of the different 12 vertex *arachno* carboranyl ligands involved in the coordination polymers (**85**)–(**91**). Vertices correspond to B–H while the circles to the  $C_c$  atom.

The *nido* carborane in polymer (**84**) can accept two electrons from sodium to become the *arachno* species resulting in the isolation of polymer (**86**)  $[\{\eta^5:\eta^7\text{-}[\text{Me}_2\text{Si}(\text{C}_9\text{H}_6)(\text{C}_2\text{B}_{10}\text{H}_{11})]\text{Er}\}_2\text{-}\{\text{Na}_4(\text{THF})_8\}]_n$ ,<sup>53</sup> whose asymmetric unit contains two  $[\eta^5:\eta^7\text{-}\text{Me}_2\text{C}(\text{C}_9\text{H}_6)(\text{C}_2\text{B}_{10}\text{H}_{11})]\text{Er}^{2-}$  synthons that are linked *via* B–H...Na bonds forming a polymeric chain (Fig. 26). The same polymer containing Dy,  $[\{\text{Me}_2\text{Si}(\text{C}_9\text{H}_6)(\text{C}_2\text{B}_{10}\text{H}_{11})\}\text{Dy}\}_2\{\text{Na}_4(\text{THF})_8\}]_n$  (**87**) (Fig. 27), is obtained by reaction of  $\text{Me}_2\text{Si}(\text{C}_9\text{H}_7)(\text{C}_2\text{B}_{10}\text{H}_{11})$  with excess of NaH in THF followed by addition of  $\text{DyCl}_3$  in excess of Na.<sup>53</sup> The two infinite polymeric chains are isostructural and isomorphous. X-ray analyses reveal a similar structure between these polymers and the polymer (**85**).<sup>54</sup> The average Ln–C( $C_5$  ring), Ln–C(cage) and Ln–B(cage) distances in (**86**) and (**87**) are longer than the corresponding values found in its cyclopentadienyl analogue of  $[\{\eta^5:\eta^7\text{-}\text{Me}_2\text{C}(\text{C}_5\text{H}_4)(\text{C}_2\text{B}_{10}\text{H}_{11})\}\text{Er}\}_2\{\text{Na}_4(\text{THF})_9\}]_n$  (**85**).<sup>54</sup>

These results indicate that the substituents indenyl or cyclopentadienyl, on carborane cage carbons may affect the overall molecular structures of the 13-vertex *closo*-metallacarborane complexes, but have little influence on the interactions between the central metal ion and the *nido*- or *arachno*-carborane ligand.

The presence of other substituents on the carborane ligands such as  $\text{Me}_2\text{NCH}_2\text{CH}_2\text{-}$  and  $\text{MeOCH}_2\text{CH}_2\text{-}$  leads to the isolation of a new class of 13-vertex *closo*-metallacarboranes.<sup>55</sup> Treatment of 1-( $\text{Me}_2\text{NCH}_2\text{CH}_2\text{-}$ )-1,2- $\text{C}_2\text{B}_{10}\text{H}_{11}$  with excess of Na in THF,

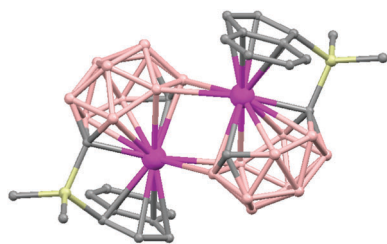


**Fig. 26** Molecular structure of  $[\{\eta^5:\eta^7\text{-}[\text{Me}_2\text{Si}(\text{C}_9\text{H}_6)(\text{C}_2\text{B}_{10}\text{H}_{11})]\text{Er}\}_2]^{4-}$  in (**86**). H atoms omitted for clarity.

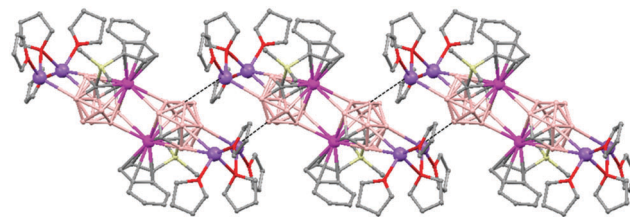


**Fig. 27** A portion of infinite polymeric chain of (**87**) (H atoms omitted for clarity).

followed by reaction with 1 equiv. of  $\text{YCl}_3$  afforded the polymeric compound  $[\{\eta^1:\eta^7\text{-}[(\text{Me}_2\text{NCH}_2\text{CH}_2)\text{C}_2\text{B}_{10}\text{H}_{11}]\text{Y}(\text{THF})\}\{\text{Na}(\text{THF})_2\}]_n$ , (**88**), (Fig. 28). A similar synthetic process using 1,2-( $\text{Me}_2\text{NCH}_2\text{CH}_2$ )<sub>2</sub>-1,2- $\text{C}_2\text{B}_{10}\text{H}_{10}$  or 1- $\text{Me}_2\text{NCH}_2\text{CH}_2$ -2- $\text{MeOCH}_2\text{CH}_2$ -1,2- $\text{C}_2\text{B}_{10}\text{H}_{10}$  with  $\text{LnCl}_3$ , (Ln = Y, Eu) leads to the formation of  $[\{\eta^1:\eta^1:\eta^7\text{-}[(\text{Me}_2\text{NCH}_2\text{CH}_2)_2\text{C}_2\text{B}_{10}\text{H}_{10}]\text{Y}\}\{\text{Na}(\text{MeCN})_2\}]_n$ , (**89**),  $[\{\eta^1:\eta^1:\eta^7\text{-}[(\text{Me}_2\text{NCH}_2\text{CH}_2)(\text{MeOCH}_2\text{CH}_2)\text{C}_2\text{B}_{10}\text{H}_{10}]\text{Y}\}\{\text{Na}(\text{MeCN})\}]_n$  (**90**) or  $[\{\eta^1:\eta^1:\eta^7\text{-}[(\text{Me}_2\text{NCH}_2\text{CH}_2)(\text{MeOCH}_2\text{CH}_2)\text{C}_2\text{B}_{10}\text{H}_{10}]\text{Er}\}\{\text{Na}(\text{MeCN})(\text{THF})\}]_n$  (**91**) after recrystallization from MeCN/toluene/THF. In all compounds, each rare earth metal ion is  $\eta^7$ -bound to the *arachno*-carboranyl ligand and  $\sigma$ -bound to two B–H vertices from the open face of the neighboring *arachno*-carboranyl cage, and coordinated to one nitrogen atom of the pendant amido substituent and one THF solvent molecule in (**88**) (Fig. 28) whereas in compounds (**89**–**91**) one  $\text{DCH}_2\text{CH}_2$  moiety (D =  $\text{Me}_2\text{N}$  or  $\text{MeO}$ ) is replaced by one THF molecule (Fig. 29). These results show that the coordination of the second side arm,

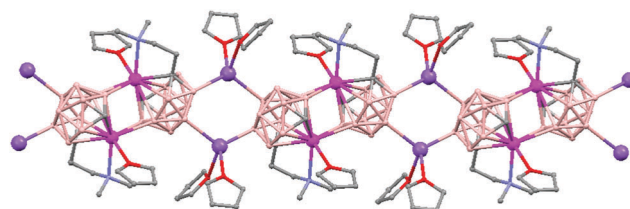


**Fig. 28** A portion of the infinite polymeric chain of (**88**). H atoms omitted for clarity.

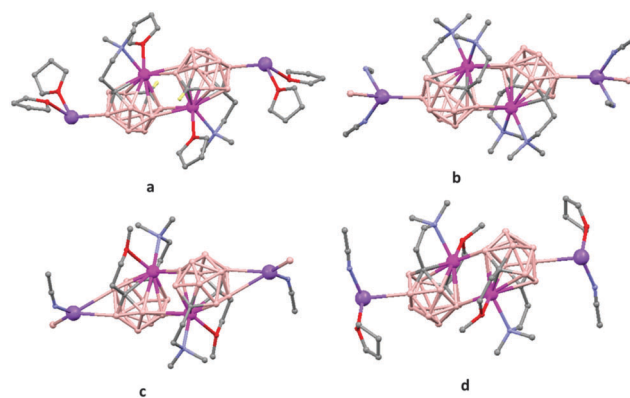


**Fig. 29** A portion of the infinite polymeric chains of (**88**–**91**) (a–d). H atoms omitted for clarity.

either Me<sub>2</sub>N or MeO, does not largely alter the basic structural unit and the overall coordination environments around the lanthanide ions. The lower number of solvent molecules around Na, less than three, probably leads to the formation of polymeric chains.

## VI. Conclusions and outlook

The incorporation of icosahedral boron clusters to  $\pi$ -conjugated polymers improves their stability and solubility and clearly alters their electrochemical, photoluminescence and electrochromic properties. The PPy films doped with anionic boron clusters act as a cation exchanger with the media, and therefore, are excellent candidates for the implementation of selective ion exchange resins controlled by an electrochemical potential. Furthermore, metallacarborane doping agents show the highest ORL of these materials. Among them, the self-doped PPy films produce an electrical material that even after losing its electroactivity due to a high destabilizing potential recovers its electroactivity in few hours. Icosahedral boron cluster-containing silane, siloxane-acetylene, polyaryl(ether), and polyimides possess exceptional thermal, thermo-oxidative, and elastic properties making them excellent candidates for high-temperature elastomers. After pyrolysis at very high temperatures, these polymers form high thermally stable ceramics that resist oxidative degradation. Icosahedral carboranyl C<sub>2</sub>B<sub>10</sub> ligands are capable of producing fascinating motifs of coordination to metals  $\eta^7$ -,  $\eta^6$ -,  $\eta^5$ - and  $\sigma$ -, which makes them attractive for new types of unconventional coordination chemistry. In addition, icosahedral boron clusters induce unconventional properties in the supramolecular structures in which they are inserted due to the possibility of introducing hydrogen and dihydrogen bonding.

The reported results on these hybrid  $\pi$  conjugated polymers presume that boron clusters will be intervening parts in the development of organic electronics particularly for technological applications such as organic photovoltaics (OPVs), organic light-emitting diodes (OLEDs), field effect transistors (FETs), sensors, and electrochromic devices. In addition, the flexible, plastic nature of the COP materials used in electronic devices has led to the realistic promise of flexible electronics in the near future. Silane and siloxane carboranyl containing polymers are promising precursors for flame retardant materials, particularly to paper products. This would be a way to use the cellulose pulp derived from wood, nowadays that the electronic books are taking a dominant role.

The particular properties of boron cluster ligands may induce unconventional properties to coordination polymers' structures making them useful for gas storage and separation, energy conversion, catalysis, bio-medical, molecular recognition and magnetic and luminescent materials.

## Acknowledgements

This work was supported by Generalitat de Catalunya (2014/SGR/149), and MINECO (CTQ2013-44670-R and CTQ2015-66143-P).

C. V. thanks European Union (COST Action CM1302-Smart Inorganic Polymers).

## References

- 1 H. Shirakawa, E. J. Louis, A. G. MacDiarmid, Ch. K. Chiang and A. J. Heeger, *J. Chem. Soc., Chem. Commun.*, 1977, **16**, 578–580.
- 2 R. McNeill, R. Siudak, J. H. Wardlaw and D. E. Weiss, *Aust. J. Chem.*, 1963, **16**, 1056–1075 and references therein.
- 3 A. F. Diaz, K. K. Kanazawa and G. P. Gardini, *J. Chem. Soc., Chem. Commun.*, 1979, 635–636.
- 4 R. N. Grimes, *Carboranes*, Academic Press, Burlington, MA, 2nd edn, 2011.
- 5 C. Masalles, J. Llop, C. Viñas and F. Teixidor, *Adv. Mater.*, 2002, **14**, 826–829.
- 6 V. Savvateev, A. Yakimov and D. Davidov, *Adv. Mater.*, 1999, **11**, 519–585.
- 7 C. Masalles, S. Borrós, C. Viñas and F. Teixidor, *Adv. Mater.*, 2000, **12**, 1199–1202.
- 8 C. Masalles, S. Borrós, C. Viñas and F. Teixidor, *Adv. Mater.*, 2002, **14**, 449–452.
- 9 C. Viñas, M. Tarrés, P. González-Cardoso, P. Farràs, P. Bauduin and F. Teixidor, *Dalton Trans.*, 2014, **43**, 5062–5068.
- 10 S. Gentil, E. Crespo, I. Rojo, A. Friang, C. Viñas, F. Teixidor, B. Grüner and D. Gabel, *Polymer*, 2005, **46**, 12218–12225.
- 11 J. Llop, C. Masalles, C. Viñas, F. Teixidor, R. Sillanpää and R. Kivekäs, *Dalton Trans.*, 2003, 556–561.
- 12 E. Crespo, S. Gentil, C. Viñas and F. Teixidor, *J. Phys. Chem. C*, 2007, **111**, 18381–18386.
- 13 J. Mola, E. Mas-Marza, X. Sala, I. Romero, M. Rodríguez, C. Viñas, T. Parella and A. Llobet, *Angew. Chem., Int. Ed.*, 2008, **47**, 5830–5832.
- 14 B. Fabre, J. Caleb Clark and M. G. Vicente, *Macromolecules*, 2006, **39**, 112–119.
- 15 E. Hao, B. Fabre, F. R. Fronczek and M. G. Vicente, *Chem. Mater.*, 2007, **19**, 6195–6205.
- 16 S. Chayer, L. Jaquinod, K. M. Smith and M. G. Vicente, *Tetrahedron Lett.*, 2001, **42**, 7759–7761.
- 17 B. Fabre, S. Chayer and M. G. Vicente, *Electrochem. Commun.*, 2003, **5**, 431–434.
- 18 E. Hao, B. Fabre, F. R. Fronczek and M. G. H. Vicente, *Chem. Commun.*, 2007, 4387–4389.
- 19 F. Barriere, B. Fabre, E. Hao, Z. M. LeJeune, E. Hwang, J. C. Garno, E. Nesterov and M. G. H. Vicente, *Macromolecules*, 2009, **42**, 2981–2987.
- 20 V. David, C. Viñas and F. Teixidor, *Polymer*, 2006, **47**, 4694–4702.
- 21 E. M. Cansu-Ergun and A. Cihaner, *J. Electroanal. Chem.*, 2013, **707**, 78–84.
- 22 M. Asay, C. E. Kefalidis, J. Estrada, D. S. Weinberger, J. Wright, C. Moore, A. L. Rheingold, L. Maron and V. Lavallo, *Angew. Chem., Int. Ed.*, 2013, **52**, 11560–11563.
- 23 J. H. Wright, II, C. E. Kefalidis, F. S. Tham, L. Maron and V. Lavallo, *Inorg. Chem.*, 2013, **52**, 6223–6229.





- 24 M. Tominaga, Y. Morisaki and Y. Chujo, *Macromol. Rapid Commun.*, 2013, **34**, 1357–1362 and references therein.
- 25 K. Kokado, M. Tominaga and Y. Chujo, *Macromol. Rapid Commun.*, 2010, **31**, 1389–1394.
- 26 K. Kokado and Y. Chujo, *Dalton Trans.*, 2011, **40**, 1919–1923.
- 27 K. Kokado and Y. Chujo, *Polym. J.*, 2010, **42**, 363–367.
- 28 J. Marshall, B. C. Schroeder, H. Bronstein, I. Meager, S. Rossbauer, N. Yaacobi-Gross, E. Buchaca-Domingo, T. D. Anthopoulos, N. Stingelin, P. Beavis and M. Heeney, *Macromolecules*, 2014, **47**, 89–96.
- 29 J. J. Peterson, M. Werre, Y. C. Simon, E. B. Coughlin and K. R. Carter, *Macromolecules*, 2009, **42**, 8594–8598.
- 30 A. R. Davis, J. J. Peterson and K. R. Carter, *ACS Macro Lett.*, 2012, **1**, 469–472.
- 31 Y. C. Simon, J. J. Peterson, C. Mangold, K. R. Carter and E. B. Coughlin, *Macromolecules*, 2009, **42**, 512–516.
- 32 K. C. Eo, M. H. Park, T. Kim, Y. Do and M. H. Lee, *Polymer*, 2013, 6321–6328.
- 33 (a) H. M. Colquhoun, D. F. Lewis, J. A. Daniels, P. L. Herbertson, J. A. H. MacBride, R. Stephenson and K. Wade, *Polymer*, 1997, 2447–2453 and references therein.
- 34 T. Xing and K. Zhang, *Polym. Int.*, 2015, **64**, 1715–1721.
- 35 L. Liang, A. Rapakousiou, L. Salmon, J. Ruiz, D. Astruc, B. P. Dash, R. Satapathy, J. W. Sawicki and N. S. Hosmane, *Eur. J. Inorg. Chem.*, 2011, 3043–3049.
- 36 S. R. Benhabbour, M. C. Parrott, S. E. A. Gratton and A. Adronov, *Macromolecules*, 2007, **40**, 5678–5688.
- 37 Y. C. Simon, C. Ohm, M. J. Zimny and E. Bryan Coughlin, *Macromolecules*, 2007, **40**, 5628–5630.
- 38 M. K. Kolel-Veetil, H. W. Beckham and T. M. Keller, *Chem. Mater.*, 2004, **16**, 3162–3167 and references therein.
- 39 M. K. Kolel-Veetil and T. M. Keller, *J. Polym. Sci., Part A: Polym. Chem.*, 2006, **44**, 147–155.
- 40 M. K. Kolel-Veetil, D. D. Dominguez, C. A. Klug, K. P. Fears, S. B. Qadri, D. Fragiadakis and T. M. Keller, *J. Polym. Sci., Part A: Polym. Chem.*, 2013, **51**, 2638–2650.
- 41 Y. Jiang, X. Li, F. Huang, Y. Zhou and L. Du, *J. Macromol. Sci., Part A: Pure Appl. Chem.*, 2015, **52**, 476–484 and references therein.
- 42 H. Kimura, K. Okita, M. Ichitani, T. Sugimoto, S. Kurok and I. Ando, *Chem. Mater.*, 2003, **15**, 355–362 and references therein.
- 43 C. E. Housecroft, *J. Organomet. Chem.*, 2015, **798**, 218–228.
- 44 G. Zi, H.-W. Li and Z. Xie, *Organometallics*, 2002, **21**, 5415–5427.
- 45 L. Deng, M.-S. Cheung, H.-S. Chan and Z. Xie, *Organometallics*, 2005, **24**, 6244–6249.
- 46 K. Chui, H.-W. Li and Z. Xie, *Organometallics*, 2000, **19**, 5447–5453.
- 47 J. H. Wrigh, G. W. Mueck, F. S. Tham and C. A. Reed, *Organometallics*, 2010, **29**, 4066–4070.
- 48 I. Rojo, F. Teixidor, C. Viñas, R. Kivekäs and R. Sillanpää, *Chem. – Eur. J.*, 2004, **10**, 5376–5387.
- 49 M. Fontanet, M. Rodríguez, I. Romero, X. Fontrodona, F. Teixidor, C. Viñas, N. Aliaga-Alcalde and P. Matějček, *Dalton Trans.*, 2014, **43**, 7838–7841.
- 50 M. Fontanet, M. Rodríguez, X. Fontrodona, I. Romero, F. Teixidor, C. Viñas, N. Aliaga-Alcalde and P. Matějček, *Chem. – Eur. J.*, 2014, **20**, 13993–14003.
- 51 S. Wang, H.-W. Li and Z. Xie, *Organometallics*, 2004, **23**, 2469–2478.
- 52 R. Khattar, M. J. Manning, C. B. Knobler, S. E. Johnson and M. F. Hawthorne, *Inorg. Chem.*, 1992, **31**, 268–273.
- 53 S. Wang, Y. Wang, M.-S. Cheung, H.-S. Chan and Z. Xie, *Tetrahedron*, 2003, **59**, 10373–10380.
- 54 K. Chui, Q. Yang, T. C. W. Mak and Z. Xie, *Organometallics*, 2000, **19**, 1391–1401 and references therein.
- 55 M.-S. Cheung, H.-S. Chan and Z. Xie, *Organometallics*, 2005, **24**, 4468–4474.

